

Mitochondrial Dynamics and Autophagy in the Hippocampus of Animal Model of Cognitive Aging

加齢性記憶障害モデル動物の海馬における
ミトコンドリアダイナミクスおよび
ミトコンドリアオートファジー

July 2020

Kosuke KATAOKA
片岡 孝介

Mitochondrial Dynamics and Autophagy
in the Hippocampus of Animal Model
of Cognitive Aging

加齢性記憶障害モデル動物の海馬における
ミトコンドリアダイナミクスおよび
ミトコンドリアオートファジー

July 2020

Waseda University

Graduate School of Advanced Science and Engineering

Department of Life Science and Medical Bioscience

Research on Solid State Bioscience

Kosuke KATAOKA

片岡 孝介

Table of content

Chapter 1. General introduction	4
1.1. Mitochondria and aging	4
1.1.1. Introduction	4
1.1.2. The free radical theory of aging	5
1.1.3. Mitochondrial DNA	6
1.1.4. Mitochondrial unfolded protein response	8
1.1.5. Mitochondrial autophagy (mitophagy)	9
1.1.6. Mitochondrial fusion and fission	11
1.2. Endocannabinoid system (ECS)	15
1.2.1. Introduction	15
1.2.2. Cannabinoids	16
1.2.3. Cannabinoid receptors	18
1.2.4. CB1 receptor and metabolism	19
1.3. Aim of this thesis	21
Chapter 2. Materials and Methods	22
2.1. Animals	22

2.2. Tissue preparation	22
2.3. Immunofluorescence staining	23
2.4. Immunofluorescence imaging	24
2.5. Conventional transmission electron microscope (TEM)	25
2.6. Focus ion beam-scanning electron microscope (FIB/SEM)	25
2.7. Mitochondrial morphological analysis	27
2.8. Statistics	27
Chapter 3. Results	28
3.1. Measuring <i>in vivo</i> mitophagy in the mouse hippocampus	28
3.1.1. Introduction	28
3.1.2. Results	32
3.1.3. Discussion	47
3.1.4. Conclusion	49
3.2. Age-dependent dual functions of cannabinoid CB1 receptor in mitochondrial dynamics and autophagy	50
3.2.1. Introduction	50
3.2.2. Results	54
3.2.3. Discussion	71
3.2.4. Conclusion	76

Chapter 4. Conclusion and Future Prospects	78
References	83
Acknowledgement	105

Chapter 1. General Introduction

1.1. Mitochondria and aging

1.1.1. Introduction

Aging is generally defined as a condition in which a continuous decline of physiological integrity of various organs, leading to increased susceptibility to diseases and death¹. The decline in functional capacity of tissues and organs can be due to a gradual loss of functional cells in tissues along the aging. Thus, open questions in this field study is what is driving force of aging. The first important study of aging emerged in 1983, in which long-lived strains of free-living nematode *Caenorhabditis elegans* was screened and isolated². Nowadays, we know much about the machinery of aging. One of the most probable machinery of aging is growing occurrence of mitochondrial dysfunction which stem from mutational mitochondrial DNA (mtDNA)^{3,4}. Mitochondrial quality must be strictly surveyed, as mitochondria regulate a number of biological processes, such as ATP generation, lipid metabolism, iron–sulfur cluster biogenesis, calcium homeostasis, and apoptosis⁵. Therefore, mitochondrial quality control system in the cell has been intensively studied since more than half a century ago. In this section, current knowledge of the relationships between mitochondria and aging process will be described.

1.1.2. The free radical theory of aging

The free radical theory of aging, proposed by Harman in 1956, suggests that aging process and aging-associated diseases may be due to the detrimental effect of reactive oxygen species (ROS) generated from mitochondria⁶. This theory predicts that a vicious cycle causes aging process. First, ROS produced by normal metabolism of mitochondrial electron transport chain (ETC) induces damage to mitochondrial macromolecules, such as proteins, DNA and lipids. Next, mutations in mtDNA in turn lead to functional impairment in subunits in the ETC. Finally, this impairment results in augmented ROS generation. Indeed, massive amount of studies have showed the positive correlation between ROS production and aging process to support this free radical theory of aging^{7,8}. However, these studies do not exclude the possibility that mitochondrial damage and ROS production are just consequences of aging process, rather than driving force of aging.

Recent studies have led us to reconsider the free radical theory of aging. For example, in studies using *Saccharomyces cerevisiae* and *C. elegans*, genetic and pharmacological intervention inactivating enzymatic anti-oxidants such as superoxide dismutase (SOD) and catalase, leads to the increased ROS production, but prolongs their life span⁹⁻¹¹. Moreover, mice deficient in mitochondrial SOD or glutathione peroxidase-1 show increased oxidative stress and incidence of pathology such as cancer, but does not accelerate aging^{12,13}. To support these studies, overexpression of enzymatic anti-oxidants SOD or catalase in mice does not extend life span¹⁴. Importantly, mice model genetically manipulated to significantly accumulate somatic mtDNA mutations shows premature aging, but does not displays increased ROS production¹⁵⁻¹⁷. Physiological levels of ROS are reported to provide a

protective role in *C. elegans*¹⁸. However, it is also reported that when ROS is beyond a certain level, ROS betrays its original physiological role and then induces aging-associated damage, ultimately causing apoptotic cell death^{17,19,20}. Collectively, these studies force a reconsideration of the role of ROS production in aging process, and establish a new conceptual framework that ROS is a stress-induced compensatory homeostatic signal for cell survival, rather than a driving force of aging.

1.1.3. Mitochondrial DNA (mtDNA)

Mitochondria contain small and circular DNAs, which are distinct from nuclear genome DNAs. Mammalian mtDNA generally encodes 13 proteins, 22 transfer RNAs and 2 ribosomal RNAs. Mitochondrially encoded proteins are all subunits for then ETC. mtDNA has been considered to be vulnerable to aging-associated somatic mutations²¹. Indeed, the amount of mtDNA mutations increases with advancing age in various tissues and organs. For instance, partial deletion of mtDNA are observed in substantia nigral neurons of aged human and patients with Parkinson's disease (PD), which is aging-related neurodegenerative disease^{22,23}. Furthermore, mtDNA point mutations accumulates in control region for replication in mtDNA in age-dependent manner^{24,25}. Since mtDNA exists in hundreds to thousands of copies per cell, coexistence of mutated and wild type mtDNA within a same cell (known as heteroplasmy) does not necessarily lead to respiratory chain dysfunction. However, the mutational loads of individual cell become significant in a poorly understood mechanism, and may gain a state of homoplasmy in which one mutated mtDNAs dominate as a result of clonal expansion of one mutated mtDNA²⁶. One of the suggested mechanisms is mitotic

segregation of mtDNA mutations. As the replication of mtDNA is not linked to the cell cycle²⁷, a particular mtDNA may be replicated many times or not at all in a cell division. During mitosis, mtDNAs are generally thought to be distributed randomly between the daughter cells²⁸. Thus, the daughter cells obtain greatly different levels of mutated mtDNA load after repeated cell divisions. It is also important to recognize that mtDNA is replicated in postmitotic cells such as neurons, and thus can undergo similar types of segregation in the absence of cell division²⁹. A heteroplasmic mtDNA mutation only causes dysfunction in ETC if present above a certain minimal threshold level, but this threshold depends on the type of mutation and affected tissue⁴.

Strongest evidence for a potential causative role for mtDNA mutations in aging comes from analyzing what is called “mitochondrial mutator mice”. This model is knock-in mice model containing a mutated (D257A), proof-reading deficient form of mtDNA polymerase POL γ . This animal model exhibits a significant level of mitochondrial mutations, respiratory chain dysfunction and accelerated aging¹⁶. Notably, ROS production and extent of oxidative stress are not upregulated¹⁷. Interestingly, mtDNA mutation load already reaches a sufficiently high level by 2 months and is unchanged during life in mutator mice, suggesting that most of the accumulated mutations may occur during embryonic and/or fetal development¹⁶. Since cells undergoing apoptosis are upregulated in multiple tissues and organs of mutator mice with aging¹⁷, it is possible that cells with a significantly accumulated mtDNA mutations beyond a critical threshold level undergo apoptosis. From these points, apoptosis and subsequent loss of irreplaceable cells may be critical for aging in mammals. In agreement with this hypothesis, caloric restriction, known as the only non-genetic intervention to

slow down aging process across a variety of species, inhibits the accumulation of mtDNA mutations load³⁰ and mitochondria-mediated apoptotic pathway³¹.

1.1.4. Mitochondrial unfolded protein response

mtDNA mutations can lead to accumulation of misfolded proteins within mitochondria, which in turn impairs mitochondrial function and ultimately cellular bioenergetic homeostasis. Thus, mitochondrial protease such as Lon protease deals with these toxic proteins³². However, during aging, gene expression of Lon protease is reduced in murine muscle³³. Further, increased expression of Lon protease extend lifespan in *Podospora anserina*, a well-known aging model in fungi³⁴. In addition to Lon protease, other mitochondrial proteases and chaperones also participate in preserving mitochondrial proteostasis to avoid excessive stresses stemming from mtDNA mutations³⁵.

However, recent studies also suggest that modest impairment in mitochondrial function could be rather beneficial for cell homeostasis. Several studies using *C. elegans* find that a modest decline or impairment in mitochondrial function leads to lifespan extension^{36,37}. Additionally, knockdown of nuclear-encoded cytochrome c oxidase subunit in *C. elegans* (*cco-1*) leads to the increase in longevity³⁶. Moreover, knockdown of a component of complex I in the ETC in *Drosophila* muscle preserves the age-dependent muscle atrophy and prolongs life span³⁸. In these animals with impairment in ETC, mitochondrial unfolded protein response (UPR^{mt}) is upregulated³⁹, which is a stress response reaction in mitochondria. During UPR^{mt}, various nuclear genome-encoded mitochondrial stress response proteins are upregulated. UPR^{mt} is generally upregulated by

accumulation of mtDNA mutations or misfolded protein within mitochondria, and triggers mitochondrial chaperone and protease. However, it is important to note that this pathway is incompletely characterized at present, and there is evidence suggesting that upregulation of UPR^{mt} itself is not sufficient to induce the increased life span⁴⁰.

1.1.5. Mitochondrial autophagy (mitophagy)

Macroautophagy (hereafter referred to as autophagy) is a highly conserved intracellular degradation system in eukaryotes, in which cytoplasmic constituents are delivered into lysosomes. Although autophagy had been thought to be non-selective degradation system for utilization of the degraded products under nutrient starvation⁴¹, recent studies have suggested that autophagy is also a highly selective process for the degradation of damaged organelle, aggregated proteins and intracellular bacteria⁴². Mitochondrial autophagy (mitophagy) is a well-documented process in which damaged or superfluous mitochondria are removed via autophagy in selective or non-selective manner (**Fig.1.1.5.1**). During mitophagy, damaged or superfluous mitochondria are sequestered in double membrane structure, so-called autophagosome, followed by fusion with lysosome containing various degradative enzymes (**Fig.1.1.5.1**). Mitochondria are first found in lysosomes in a study using electron microscope in 1957⁴³, which was the first study indicating the existence of mitophagy. Today, the detailed molecular mechanisms involving mitophagy have been revealed⁴⁴, which is mostly based on intensive *in vitro* research.

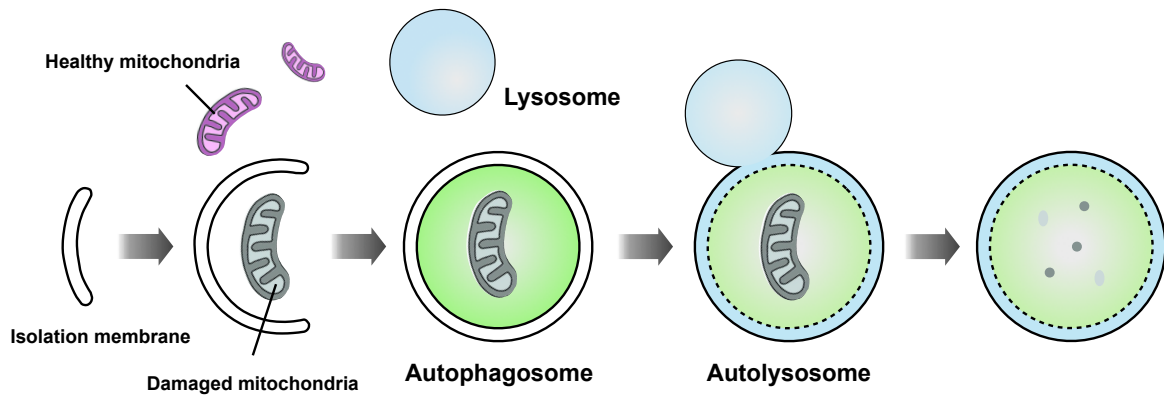


Fig. 1.1.5.1. Graphical overview of mitophagy

When the amount of misfolded proteins stemming from mtDNA mutations or proteotoxic stress accumulate to a level that exceeds the UPR^{mt} capacity, or the mitochondrial membrane potential is disrupted, mitophagy appears to play an important role in preserving cellular energy homeostasis. Mitophagy activity is reduced in hippocampal dentate gyrus (DG) of aged mice⁴⁵ and hippocampus of patients with aging-related neurodegenerative diseases such as Alzheimer's disease⁴⁶. Furthermore, pharmacological forced induction of mitophagy alleviates symptoms of Alzheimer's disease in mouse model⁴⁶, and prolongs lifespan in *C. elegans*⁴⁷.

Although mitophagy has multiple pathways, phosphate and tensin homolog (PTEN)-induced putative kinase 1 (PINK1) and Parkin are well-characterized molecules in selective mitophagy. These genes are associated with a recessive type of early onset PD^{48,49}, known as a selective aging-associated loss of dopaminergic neurons and motor dysfunction. PINK1 and Parkin function in a common signaling pathway that is important for executing efficient mitophagy. So far, genetic animal models targeting *PINK1* and *Parkin* gene have showed aging and aging-related

symptoms⁵⁰. For example, loss of Parkin in *Drosophila* leads to decrease in life span⁵¹. Conversely, Parkin overexpression extends fly longevity⁵². *Drosophila PINK1* null mutant displays shortened lifespan and high sensitivity to various stresses⁵³. Although neither POL γ mutator mice nor Parkin null mice show loss of dopaminergic neurons, mutator mice in the background of Parkin deficiency show age-dependent loss of dopaminergic neurons in substantia nigra⁵⁴.

Another link between mitophagy-related molecule and lifespan is being proposed. Interestingly, Lon protease modulates PINK1 levels in mitochondria⁵⁵, suggesting the existence of cross-interaction among different layers of mitochondrial quality control. These findings propose that mitophagy could be tightly associated with aging speed.

1.1.6. Mitochondrial fusion and fission

Mitochondrial morphology is determined by well-coordinated fusion and fission processes. Mitochondrial morphologies vary greatly by cell type and tissue. For example, mitochondria are long filament in fibroblast, while hepatocytic mitochondria show uniform and spherical morphology⁵⁶. A large group of GTPases mediate mitochondrial these processes. Their combinational actions drive fission and fusion of two lipid bilayers (inner-membrane and outer-membrane) that surround mitochondria.

In fission process, cytosolic dynamin related protein 1 (Drp1) assembles into polymers that encircle around the surface of mitochondria. Drp1 then drives mitochondrial constriction by mechanochemical force through GTP hydrolysis⁵⁷. In many fission events, daughter mitochondrion

is often polarized, while the sister mitochondrion is depolarized and degraded by mitophagy⁵⁸ (**Fig. 1.1.6.1**). In addition, mitophagy is impaired by overexpression of dominant negative form of Drp1⁵⁸. In mice lacking the key autophagy gene *Ulk1* or *Atg7*, swollen and dysfunctional mitochondria accumulates in the cells^{59,60}. Although recent studies suggest that Drp1 is not necessarily required by mitophagy^{61,62}, it is no wonder that mitochondrial fission is important for efficient mitophagy in various cell types. Drp1 also participates in mitochondria-associated apoptosis⁶³. During apoptosis, pro-apoptotic Bcl-2 family member Bax moves from cytosol to mitochondrial outer-membrane, and cytochrome c is released from mitochondria, which triggers apoptosis. Drp1 knock-down is shown to delay the release of cytochrome c and inhibits apoptotic cell death⁶³.

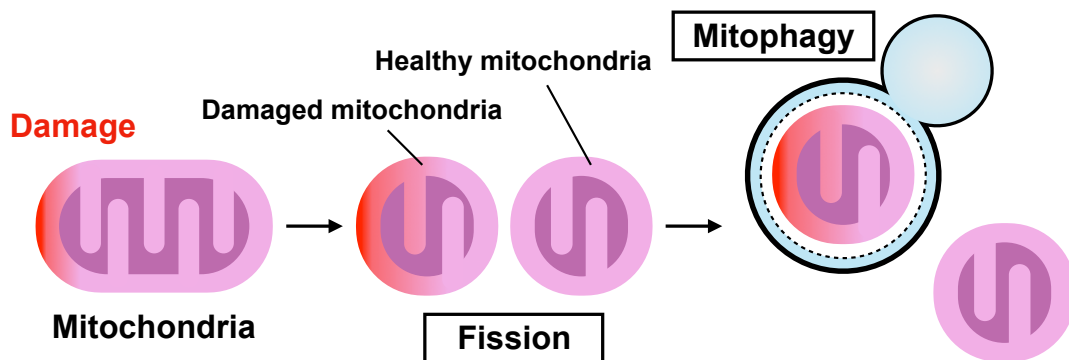


Fig. 1.1.6.1. Mitochondrial fission contributes to removal of damaged part of mitochondria

In fusion process, mitochondrial inner-membrane and outer-membrane are fused in separate mechanisms. The fusion between inner-membranes is mediated by a single dominant dynamin family member called optic atrophy protein 1 (OPA1), while fusion between outer-

membrane is mediated by two members, mitofusin 1 and 2 (Mfn1 and Mfn2) in mammals. Mitochondrial fusion is helpful for stress response, in which healthy and functional mitochondria complement damaged and dysfunctional mitochondria by diffusion and sharing damaged components such as mutated mtDNAs and misfolded proteins (**Fig. 1.1.6.2**). Extracellular stress or starvation induces mitochondrial hyper-elongation (often called stress-induced mitochondrial hyperfusion, SIMH)^{64,65}, which is proposed to protect mitochondria from autophagy-induced degradation to maintain oxidative phosphorylation and produce ATP⁶⁵. Mitochondrial fusion is well-characterized in cell senescence. Several studies suggest that forced induction of mitochondrial fusion by pharmacological and genetical tools can lead to increased ROS and cell senescence^{66,67}.

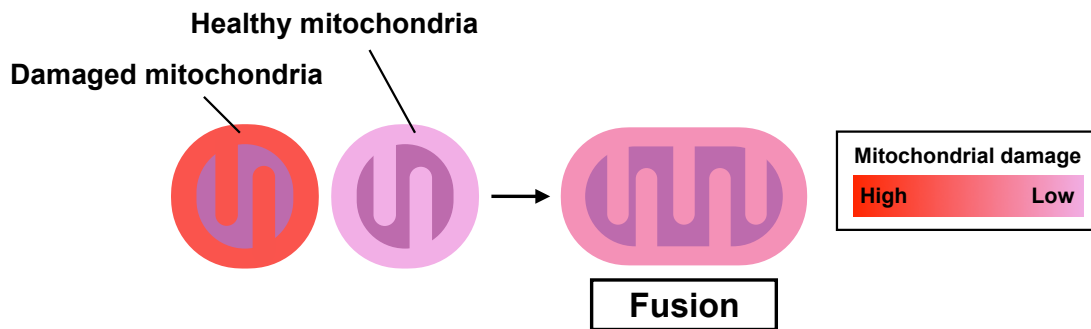


Fig. 1.1.6.2. Mitochondrial fusion contributes to alleviation of detrimental effects of damaged mitochondria

Overall, these previous studies suggest that well-coordinated fission and fusion process is critical for mitochondria quality control and cellular energy homeostasis. Perturbation or imbalance

between fission and fusion can lead to detrimental impacts on the proper functions of cells and even fate for cell survival.

1.2. Endocannabinoid system (ECS)

1.2.1. Introduction

The ECS comprises lipid-based ligands (endocannabinoids), their receptors (cannabinoid receptor type 1, or CB1 receptor and cannabinoid receptor type 2, or CB2 receptor) and enzymes that are involved in their biosynthesis and degradation. Animal models and human studies have greatly expanded the understanding of molecular mechanism of the ECS, and demonstrated its involvement in physiology and pathology. As this system involves neuron, astrocyte and microglia in the central nervous system (CNS) (**Fig. 1.2.1.1**), the complex signaling among these cells gives rise to various neurological functions such as memory, moods, appetite, seizure and chronic pain⁶⁸. In addition to the functions in the CNS, the ECS is widely prevalent in the body and regulates energy homeostasis in a large number of organs and tissues⁶⁹. Thus, the components of the ECS is considered as the promising potential therapeutic target for a wide range of disorders including type 2 diabetes, chronic pain, cardiovascular diseases and neurodegenerative diseases⁷⁰. Notably, accumulating evidence suggests that the ECS tone is tightly associated with aging-associated cognitive decline⁷¹. In this section, the current knowledge on the ECS and its physiological and pathological significance will be described.

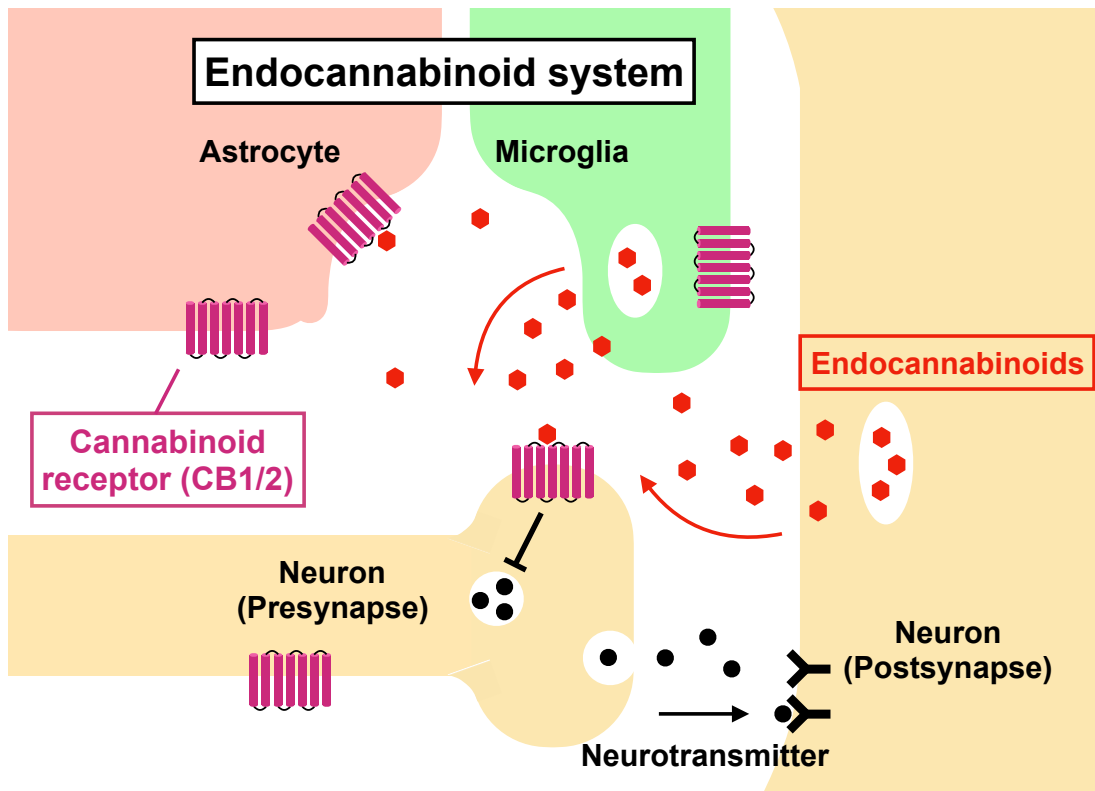


Fig. 1.2.1.1. Endocannabinoid system

1.2.2. Cannabinoids

Cannabis sativa, also known as marijuana, has been used for various purposes, such as recreation and medicine, from antiquity. The cannabis plant contains more than 60 biologically active compounds, which are so-called cannabinoids⁷². Δ^9 -tetrahydrocannabinol (THC) and cannabidiol (CBD) are most abundant molecules of plant-derived cannabinoids, and have been intensively investigated because they have a plenty of beneficial and adverse effects. The chemical structures of THC and CBD are shown in Fig. 1.2.2.1. Although these cannabinoids share most of molecular structure, their biological impacts are different and complex. For example, THC is responsible for

dose-dependent development of memory impairment, hypoactivity and hypothermia, whereas CBD does not have such effects⁷³. Additionally, it is also reported that CBD enhances the pharmacological effects of THC⁷³.

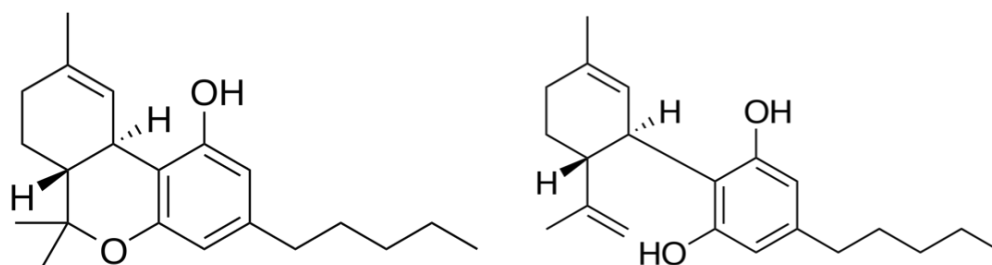


Fig. 1.2.2.1. Chemical structures of THC (left) and CBD (right)

In addition to the plant-derived cannabinoids, cannabinoids also have two classes of cannabinoids: the endocannabinoids and synthetic cannabinoids. *N*-arachidonoyl-ethanolamine (anandamide) and 2-arachidonoyl-glycerol (2-AG) are the two well-documented endocannabinoids. The chemical structures are shown in **Fig. 1.2.2.2**. These endocannabinoids are generated from phospholipid precursors by enzymes such as *N*-acyl-phosphatidyl-ethanolamine (NAPE)-selective phospholipase D (NAPE-PLD) for anandamide⁷⁴ and diacylglycerol lipases (DAGL α and DAGL β)⁷⁵. Endocannabinoids act on cannabinoid receptors and other receptors such as transient receptor potential cation channel subfamily V member 1 (TRPV1)⁷⁶ and peroxisome proliferator-activated receptor γ (PPAR γ)⁷⁷, thus causing various biological consequences. Endocannabinoids are then imported into the cells by poorly understood mechanisms and inactivated by hydrolysis enzymes.

Fatty acid amide hydrolase 1 (FAHH) catalyzes the hydrolysis of anandamide⁷⁸, while 2-AG is hydrolyzed by monoacylglycerol lipase (MAGL)⁷⁹.

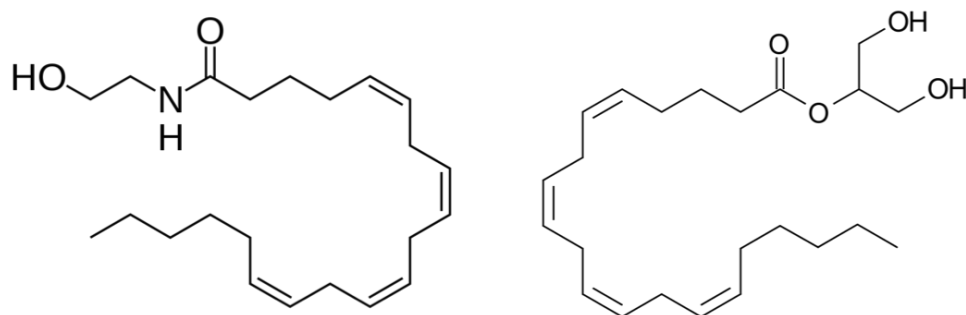


Fig. 1.2.2.2. Chemical structures of anandamide (left) and 2-AG (right)

1.2.3. Cannabinoid receptors

CB1 receptor was first discovered as a binding partner to THC in 1988, and cloned from rat brain in 1990 (encoded by *Cnr1* gene)^{80,81}. CB2 receptor was next cloned from myeloid cells in 1993 (encoded by *Cnr2* gene)⁸². CB1 receptor is thought to be mainly responsible for the biological effects of marijuana use, such as psychoactive effects⁸³. Both CB1 and CB2 receptor are seven-transmembrane G protein-coupled receptors (GPCR), which associate with G protein type $G_{i/o}$, and less frequently with the type $G_{q/11}$. This coupling promotes mitogen-activated protein kinases (MAPK), and downregulates adenylate cyclase and its downstream cyclic AMP-protein kinase A (PKA). These MAPKs include extracellular signal-regulated kinase 1 (ERK1), ERK2, p38 MAPKs and JUN N-terminal kinases (JNK)⁸⁴. CB1 receptor also inhibits neurotransmitter release in

presynaptic region by hindering L-, N- and P/Q-type voltage activated Ca^{2+} channels and stimulating inwardly rectifying K^{+} channels⁸⁵. CB1 receptor is probably the most abundant GPCR in the CNS, and predominantly expressed in the hippocampus, cortex, basal ganglia and cerebellum⁸⁶. In contrast to CB1 receptor, CB2 receptor is mainly expressed in immune cells in the periphery, yet its expression is found in neuronal, glial and endothelial cells to a lesser extent⁸⁷. In activated glial cells under neuroinflammation, expression of CB2 receptor is upregulated⁸⁷, modulating their inflammatory responses.

The Expression of CB1 receptor is mostly found in neuronal axons and presynaptic terminals of both excitatory (glutamatergic) and inhibitory (GABAergic) neurons, although a small population appears to be expressed in postsynaptic region⁸⁸. Differential roles of CB1 receptor in distinct neuronal populations have been revealed using conditional knock out mouse model⁷¹. For example, CB1 receptor on glutamatergic, but not GABAergic, neurons is indispensable for neuroprotective activity of (endo)cannabinoids⁸⁹. In contrast, CB1 activity on GABAergic neurons has been reported to protect against aging-associated cognitive decline by alleviating neurodegeneration of hippocampal pyramidal cells and neuroinflammation⁹⁰.

1.2.4. CB1 receptor and metabolism

Accumulating evidence suggest that the ECS, especially CB1 receptor, plays important roles in cellular and physiological energy metabolism. For example, mice lacking CB1 receptor are resistant to diet-induced obesity and shows leanness^{91,92}. CB1 antagonists/inverse agonists, such as

rimonabant, improve hepatic steatosis and reduce fat mass^{93,94}. These observations can be partly explained by the findings that the ECS controls motivations for food intake in hypothalamus⁹⁵. However, liver-specific deletion of CB1 receptor also shows less steatosis and insulin resistance in mice⁹⁶. These studies suggest that CB1 receptor may be involved in energy metabolism. In consistent with this, CB1 expression is observed in tissues with high energy demand. These tissues include not only brain, but also adipose tissue, liver, skeletal muscle and pancreas⁹⁶⁻⁹⁸.

Interestingly, CB1 receptor has been reported to regulate mitochondrial functions and integrities⁹⁹. Recent studies also suggest that CB1 receptor is endogenously expressed in mitochondrial membrane, not only in plasma membrane, where CB1 receptor regulates mitochondrial oxidative phosphorylation and energy production^{100,101}. These studies suggest that the ECS, especially CB1 receptor, is important for the energy homeostasis.

1.3. Aim of this thesis

Brain accounts for approximately 2% of animal body weight, yet it consumes around 20% of the glucose and oxygen of whole body to generate the energy required for brain's activity, such as maintaining ionic gradient across the cell membrane and other synthetic processes¹⁰². As described in the previous sections, CB1 receptor plays important roles in maintaining energy metabolism. Mitochondria are responsible for producing most of cellular energy, especially in tissues with high metabolic demand, such as brain. Therefore, it is conceivable that CB1 receptor might regulate mitochondrial integrity to maintain energy homeostasis and brain's physiological functions. However, it is unknown whether CB1 receptor has functions in mitochondrial quality control system in mammalian tissues such as brain.

This thesis aims to investigate whether CB1 receptor has a role in major mitochondrial quality control system in the mouse brain. In this study, hippocampus will be focused in the following reasons; hippocampus shows abundant CB1 receptor expression⁸⁶ and mice lacking CB1 receptor shows age-dependent memory decline and hippocampal neurodegeneration^{90,103}.

Chapter 2. Materials and Methods

2.1. Animals

For the experiments of PINK1, brains obtained from *PINK1*^{-/-} mice (PINK1-KO) and *PINK1*^{+/+} mice (WT) (aged 7 months) were kindly gifted by Dr. Miratul Muqit (MRC Protein Phosphorylation Unit, University of Dundee) and stored at -80°C until further processing. The animals used in all experiments were mix-gendered. PINK1-KO were generated as described previously¹⁰⁴.

For the experiment of CB1 receptor, young (1-2 months old) and adult (6-7 months old) mix-gendered animals on a congenic C57BL6/J background were used. Animals received water and food ad libitum. Mice were housed in groups of three to five and kept in a temperature (21 ± 1 °C) and humidity (55 ± 10%) controlled room with a reversed 24 hours light-dark cycle (12 hours light and 12 hours dark) at the animal facility of the Medical Faculty at the University of Bonn. For experiments using adult mice, animals were obtained from heterozygous pairs, while for those using young mice, they were from homozygous pairs. Animal experiments were approved by the local Committee on the Ethics of Animal Experiments of Landesamt fuer Natur, Umwelt und Verbraucherschutz Nordrhein-Westfalen (LANUV NRW; Permission Number: 84-02.04.2015.A265).

2.2. Tissue preparation

Brains of mice were dissected following scarification by decapitation. The brains were immediately frozen by ice-cooled isopentane and stored at -80°C until further processing. Brain samples containing the hippocampus were serially cut into $16\text{-}\mu\text{m}$ thick coronal slices using a cryostat (Leica CM 3050; Leica, Welzlar, Germany) and placed onto glass slides. Slides were stored at -80°C until staining.

2.3. Immunofluorescence staining

Frozen brain sections were put on a hot plate at 40°C for about 20 min. Sections were framed with a PapPen and post-fixed in 4% paraformaldehyde dissolved in 0.1 M phosphate-buffered saline (PBS: pH 7.3) for 30 min. After three 10-min washes in PBS, sections were permeabilized in 0.5% Triton X-100 for 1 hour, followed by three 10-min washes in PBS. Blocking of unspecific binding sites was performed by incubation in PBS containing 3% bovine serum albumin (BSA) for 2 h. The sections were then incubated with primary antibodies at 4°C overnight. The primary antibodies used in this study were as follows: a rabbit anti-phospho-ubiquitin (Ser65) antibody (Merck Millipore, Burlington, MA, USA, ABS1513-1; 1:500 in 0.3% BSA in PBS), an Alexa Fluor 488-conjugated mouse anti-NeuN antibody (Merck Millipore, MAB377X; dilution, 1:500 in 0.3% BSA in PBS) and a chicken polyclonal anti-GFAP antibody (Abcam, Cambridge, UK, ab4674; dilution, 1:200 in 0.3% BSA in PBS). Subsequently, the slides were rinsed three times for 10 min in PBS and incubated with secondary antibodies. The secondary antibodies used in this study were as follow: a goat anti-rabbit Cy3-conjugated secondary antibody (Invitrogen, Waltham,

CA, USA, 1081937; 1:1000 in 0.3% BSA in PBS; for samples from young animals) and Cy5-conjugated secondary antibody (Invitrogen, A10523; 1:1000 in 0.3% BSA in PBS; for samples from adult animals). After staining, the sections were rinsed three times for 10 min in PBS, mounted with DAPI-containing Fluoromount-G (Southern Biotech, Birmingham, AL, USA), and covered with cover slips.

2.4. Immunofluorescence imaging

To assess the colocalization of Ser65-pUb/NeuN and Ser65-pUb/lipofuscin, images were acquired using a Leica LSM SP8 confocal microscope equipped with a 60× water-immersion lens. For the analysis of Ser65-pUb-positive cells in the whole hippocampus, images were acquired using a Leica LSM SP8 confocal microscope equipped with a 20× lens in the “Tile Scan” mode. Three to four images per animal that included the whole hippocampus were obtained for analysis. The number of Ser65-pUb-positive cells in the hippocampus was counted automatically using the “Analyze particles” tool in Image J Fiji (NIH, Bethesda, MD, USA), after thresholding. For the analysis of Ser65-pUb and DAPI signal intensity in the CA3 region, images were acquired using a Leica LSM SP8 confocal microscope equipped with a 10× lens. Three to four images per sample that included the whole CA3 region were obtained for analysis. Finally, the CA3 regions in the hippocampus were framed using the “Polygon selection” tool and Ser65-pUb signal intensities were measured using Image J Fiji (NIH).

For imaging Ser65-pUb-positive cells in hippocampus in CB1-KO and WT, images were acquired using a Zeiss Axiovert 200M fluorescent microscope (Carl Zeiss Microimaging, Oberkochen, Germany) with a 20×, 0.8 NA lens. The number of Ser65-pUb-positive cells in hippocampus was manually counted using “Cell Counter” tool in Fiji software (NIH, Bethesda, MD, USA) in a blinded manner. Four to five images per animal that included the whole hippocampus were obtained for analysis.

2.5. Conventional transmission electron microscope (TEM)

Animals were intracardially perfused with 0.1 M phosphate buffer (PB), followed by Kamovsky fixative solution (2.5 % glutaraldehyde and 2 % PFA in 0.1 M PB). Brains dissected from the animals were next post-fixed in the Kamovsky fixative solution over one week. After rinsed in PB, samples were post-fixed in 1% osmium tetroxide in PB for 2 hrs at 4°C. The resulting samples were then block-stained with a saturated uranyl acetate solution and a series of ethyl alcohol. The samples were finally embedded in epoxy resin (Epon812).

Ultrathin sections were cut by an ultramicrotome (UC7k; Leica). These sections were then stained with uranyl acetate and lead citrate. Imaging was performed by H-7650 TEM (Hitachi High Technologies, Tokyo, Japan).

2.6. Focus ion beam-scanning electron microscope (FIB/SEM)

Animals were perfused, and their brains were post-fixed in the same way as TEM. The samples were then fixed with 1.5 % potassium ferrocyanide and 2 % osmium tetroxide for 1 hr at 4°C. Next, the brains were treated with 1 % triocarbonylhydrazide and then in a 2 % osmium tetroxide solution 1 hr at room temperature. The *en bloc* staining was performed for enhancing the contrast of membrane structures in cells, in which the brains were immersed in a solution of 4 % uranyl acetate overnight. The samples were further stained with Walton's lead aspartate solution. After dehydration with a stepwise ethanol series, the samples were transferred into ice-chilled acetone. Finally, they were embedded with Epon812 followed by polymerization.

The surface of the samples attached to metal stubs were trimmed by a diamond knife. Staining of semithin sections with toluidine blue was performed to check whether regions of interest were included. The sample surface charging was prevented by coating with protective layer of carbon. FIB/SEM (Scios; FEI, Hillsboro, OR, USA) was conducted after carbon deposition on the milling area. A focused gallium ion beam (accelerating voltage: 30 kV, current: 0.3 nA, milling step: 30 nm, 1,000 cycles) was used for repetitive milling. Imaging was performed by SEM as compositional contrast image from back scattered electrons. The resulting image stacks were analyzed by Avizo 8.1 (FEI, Burlington, MA, USA). Mitochondrial 3D morphology was traced in a semimanual way implemented in Avizo 8.1.

2.7. Mitochondrial morphological analysis

17-39 electron micrographs that included one to two hippocampal CA1 neuronal soma were obtained for analysis. Mitochondrial morphology was determined by using “Freehand selections” tool in Fiji software (NIH). Area, perimeter and circularity of individual mitochondria were analyzed by using “Analyze particles” tool in Fiji software (NIH).

2.8. Statistics

Statistical analysis was performed using GraphPad Prism (version 5.0 or 8.0).

To analyze the number of Ser65-pUb-positive cells in the whole hippocampus between PINK1-KO and WT, data were processed using unpaired Student’s *t*-tests with Welch’s correction, because they showed significantly unequal variances. The remaining data were analyzed using unpaired Student’s *t*-tests. **P* < 0.05, ***P* < 0.01, significant differences compared with WT counterparts.

For studies of CB1 receptor, data analysis was performed using two-way ANOVA followed by Tukey’s multiple comparison test. Statistical significance is indicated by **P* < 0.05, ***P* < 0.01, ****P* < 0.001 and *****P* < 0.0001 for age effect, and #*P* < 0.05, ##*P* < 0.01, ###*P* < 0.001 and ####*P* < 0.0001 for genotype effect. n.s. stands for not significant.

Chapter 3. Results

3.1. Measuring *in vivo* mitophagy in the mouse hippocampus

3.1.1. Introduction

The mechanism of PINK1 and Parkin-dependent mitophagy

PINK1 and Parkin play important roles in the mechanism for amplifying signal for mitophagy¹⁰⁵. The loss-of-function of them is the most common cause of hereditary early-onset PD^{48,49}, which is characterized by mitochondrial dysfunctions in brain¹⁰⁶. Here, the mechanism of PINK1 and Parkin-dependent mitophagy will be described. Graphical overview is shown in **Fig.**

3.1.1.1.

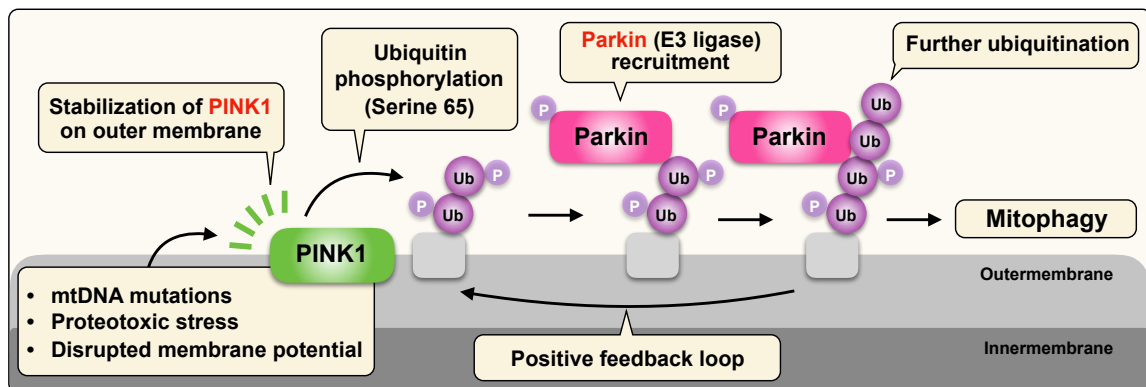


Fig. 3.1.1.1. Graphical overview of PINK1 and Parkin-dependent mitophagy

In healthy mitochondria with polarized membrane potential, after translation in the cytosol, PINK1 is imported into the mitochondrial inner-membrane, where it is degraded by mitochondrial-resident proteases⁵⁵. However, mitochondria can be damaged by accumulation of mitochondrial DNA mutations and misfolded proteins within matrix^{62,107}. These events lead to the depolarization

of mitochondrial membrane potential, and stabilization of PINK1 in the outer-membrane¹⁰⁸⁻¹¹⁰. Critically, the stabilized PINK1 phosphorylates (at Serine 65) the ubiquitin molecules that are attached to proteins in the outer-membrane¹¹¹⁻¹¹³. The resulting phosphorylated product (Ser65-pUb) recruits the E3 ubiquitin ligase Parkin from cytosol to the damaged mitochondria, where PINK1 phosphorylate the ubiquitin-like domain in Parkin to potentiate its latent E3 ligase activity¹¹⁴⁻¹¹⁷. Finally, a positive feedback loop accelerates further Parkin translocation and formation of poly-ubiquitin chains on damaged mitochondria. Amplified Ser65-pUb chains recruit various factors that are required for autophagy initiation, such as optineurin and NDP52¹⁰⁵.

The in vivo research on PINK1 and Parkin-dependent mitophagy

The detailed mechanisms underlying the PINK1 and Parkin-dependent mitophagy pathway have been intensively investigated in *in vitro* research, yet many questions remain pertaining to the existence and physiological significance of mitophagy *in vivo*. Several studies using animal models such as fruit fly and mouse have been conducted so far⁵⁰. In *Drosophila*, mitophagy is present in muscles and brain tissues in physiological conditions¹¹⁸. *Drosophila* lacking *PINK1* or *Parkin* gene exhibit abnormalities in mitochondria, neurology and behavior, which closely resemble the symptoms of human cases with PD^{51,53,119,120}. Ser65-pUb expression is also observed in dopaminergic neurons in *Drosophila*, suggesting that PINK1 and Parkin signaling functions faithfully¹²¹. Human postmortem brain specimens shows the distribution of Ser65-pUb expression throughout the brain, including the substantia nigra and hippocampus¹²². Expression level of Ser65-pUb is upregulated in

an age-dependent manner and in PD brains¹²³. Moreover, Ser65-pUb production is impaired in iPSCs derived from PD patients harboring *PINK1* and *Parkin* mutations^{121,123}. In contrast to *Drosophila*, *PINK1* and *Parkin* knockout mice fails to display PD-like pathologies, despite the presence of pronounced mitochondrial dysfunction. A reporter mouse model for *in vivo* mitophagy shows that basal mitophagy occurs independently of PINK1¹²⁴. However, a recent study using an elegant genetic mouse model highlights the significance of endogenous mitophagy activity in the mouse⁵⁴. In this study, Parkin deficient mouse model is crossed with the “POL γ mutator mice”. This mouse model shows the accumulation of Ser65-pUb in brains and PD-like pathologies⁵⁴. Although this study has demonstrated that the PINK1 and Parkin signaling at the basal level is present and important in mouse models, little is known about the *in situ* signaling activity of PINK1 and Parkin in mouse tissues.

Challenges in research on in vivo mitophagy

To study the role and prevalence of *in vivo* mitophagy in mammalian model, several mouse models have been developed; MitoQC¹²⁵, MitoKeima⁴⁵ and MitoTimer¹²⁶. The problem is that these models are not readily available to many researchers. Shortly after the discovery of Ser65-pUb, antibodies against Ser65-pUb have been developed for studying the physiological and pathological relevance of this protein in humans and fruit flies^{121,122}. Furthermore, quantitative mass spectrometry is utilized for monitoring Ser65-pUb levels in mouse tissues, yet this technique needs expertise, and more importantly, lose spatial information in mouse tissues⁵⁴. A recent study has revealed that Ser65-pUb levels positively correlate with mitophagy activity in mouse heart¹²⁷, suggesting the possible

validity of Ser65-pUb as a marker for mitophagy in tissues. Further studies are needed to fully decipher the biological roles of mitophagy in a variety of organ systems, including brain.

The aim of this section

In this section, the results of Ser65-pUb immunohistochemistry in mouse hippocampi will be described. Although Ser65-pUb is emerging as a possible biomarker of PINK1 signaling activity *in vivo*^{121,123,127}, few studies have used immunohistochemistry to analyze Ser65-pUb in the mouse. In this study the immunohistochemical characteristics of Ser65-pUb was investigated in the mouse hippocampus. First, some hippocampal cells were Ser65-pUb positive, whereas the remaining cells expressed no or low levels of Ser65-pUb. PINK1 knockout mice showed the decreased density of Ser65-pUb-positive cells, which is consistent with a previous hypothesis based on *in vitro* studies. Notably, Ser65-pUb-positive cells were detected in hippocampi lacking *PINK1* gene. The CA3 pyramidal cell layer and the dentate gyrus (DG) granule cell layer exhibited significant reductions in the density of Ser65-pUb-positive cells in PINK1-deficient mice. Furthermore, Ser65-pUb signal colocalized with neuronal markers. Collectively, Ser65-pUb may serve as a *in situ* biomarker of PINK1 signaling in the mouse hippocampus. However, the data should be interpreted carefully, as PINK1 deficiency downregulated Ser65-pUb expression only partially.

3.1.2. Results

Some cells strongly express Ser65-pUb in the hippocampus, while other cells express no or low levels of Ser65-pUb

First, the immunohistochemical characteristics of Ser65-pUb in the mouse hippocampus was investigated. As a result, some cells exhibiting strong signals were distributed throughout the hippocampus, whereas the remainder of the cells expressed no or weak Ser65-pUb in WT controls (**Fig. 3.1.2.1A**). To confirm that these immunoreactivities were the consequence of specific staining for Ser65-pUb, a genetic mouse model was used¹⁰⁴. As PINK1 catalyzes the phosphorylation of ubiquitin at Serine 65 for the execution of mitophagy¹¹¹⁻¹¹³, the effect of PINK1 deficiency on Ser65-pUb signal in the hippocampus was examined. To avoid analytical inaccuracies, unbiased image quantification was conducted. In this analysis, Ser65-pUb-positive cells in the hippocampus were counted after the application of image segmentation with the same threshold range across all images. This method revealed that PINK1 deficiency resulted in a significant reduction in the density of Ser65-pUb-positive cells in hippocampus (**Fig. 3.1.2.1B**). Interestingly, Ser65-pUb-positive cells were also detected in PINK1-KO, possibly indicating the presence of PINK1-independent phosphorylation of ubiquitin.

To corroborate the findings above, Ser65-pUb fluorescence intensities were measured in the hippocampal CA3 region. As a consequence, mean signal intensity of Ser65-pUb in the CA3 was significantly decreased in PINK1-KO compared with age-matched WT controls (**Fig. 3.1.2.2**). The DAPI signal was comparable between mice of the two genotypes, indicating that, in the hippocampus

of PINK1-KO, Ser65-pUb expression was decreased, while the cell density was unchanged compared with the WT controls (**Fig. 3.1.2.2**). These results suggest that Ser65-pUb is generated at high levels in a subset of cells of the hippocampus, which is at least partially dependent on PINK1 activity.

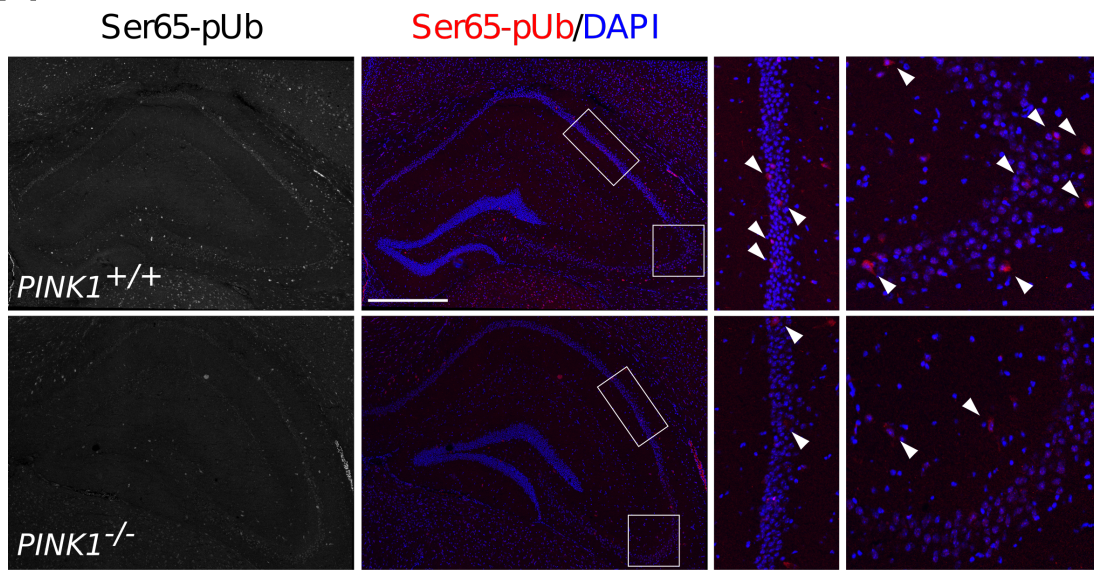
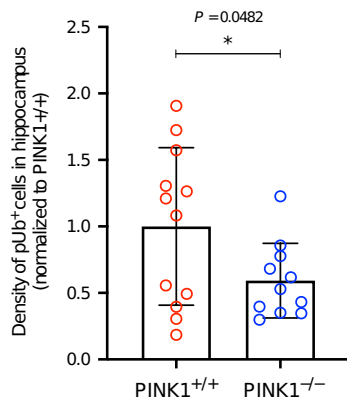
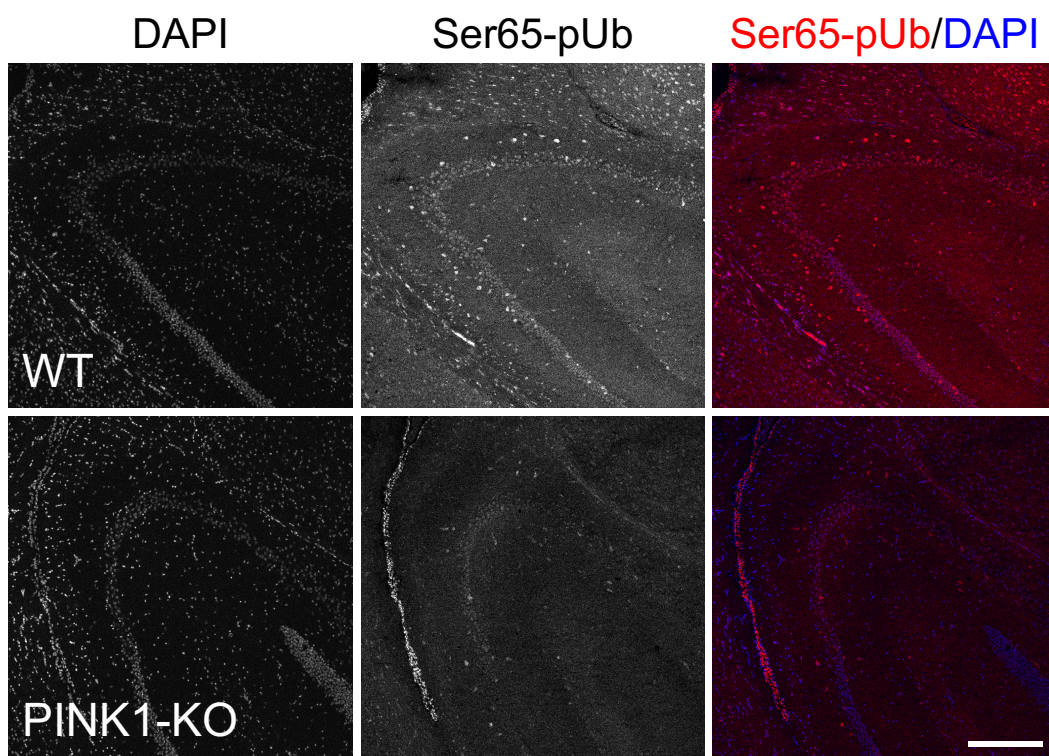
A**B**

Fig. 3.1.2.1. The density of Ser65-pUb-positive cells was decreased in PINK-KO. (A) Representative confocal microscopy images of hippocampi in PINK1-KO and WT controls. Coronal sections were immunostained with an anti-Ser65-pUb antibody (red). Nuclei were stained with DAPI (blue). Hippocampus of animals with both genotypes showed a subset of cells expressing strong Ser65-pUb signal. The boxed regions are magnified on the right. The white arrows indicate examples of cells strongly expressing Ser65-pUb. Scale bar indicates a length of 500 μ m. (B) Quantitative analysis on the density of Ser65-pUb-positive cells in the whole hippocampus in PINK1-KO and WT controls. The density of Ser65-pUb-positive cells were significantly decreased in PINK1-KO. The results are expressed as the mean \pm S.E.M. Circles represent individual value of the density of Ser65-pUb-positive cells in one section. Three animals per genotype were used in this analysis. Statistical significance is indicated by $*P < 0.05$. This figure is reprinted version from the Figure 1A and 1B of Kataoka, K. *et al.*, 2020¹²⁸.

A



B

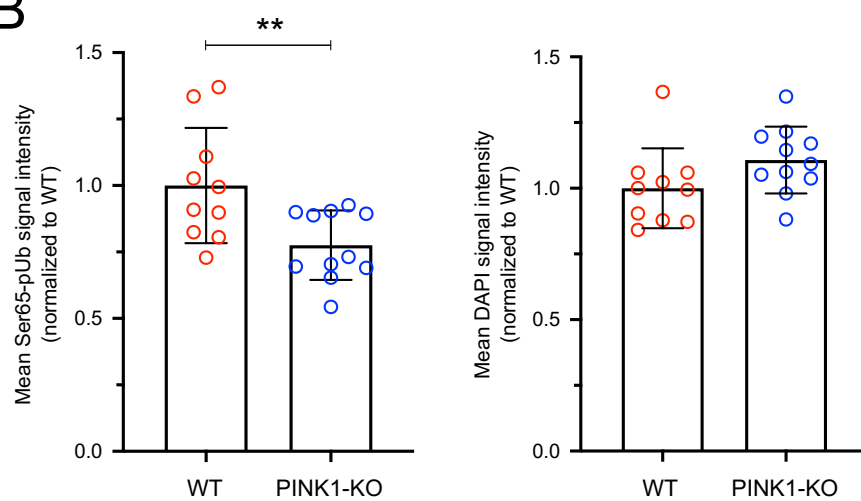
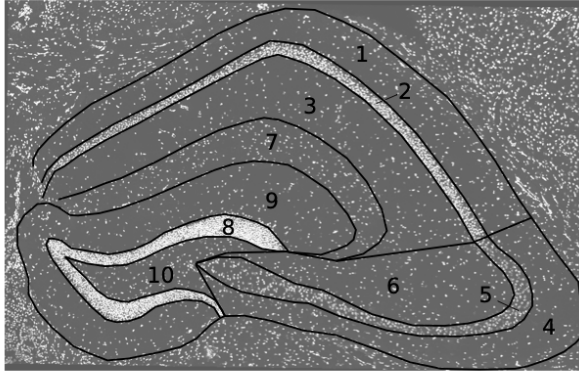


Fig. 3.1.2.2. The mean signal intensity of Ser65-pUb signal in hippocampal CA3 regions is significantly reduced in PINK1-KO compared to WT. (A) Representative confocal microscopy images of hippocampal CA3 regions in PINK1-KO and WT controls. Coronal sections were immunostained with Ser65-pUb antibody (red). Nucleus was stained with DAPI (blue). Scale bar indicates a length of 250 μm . (B) Quantitative analysis on means of fluorescence signal intensities of Ser65-pUb and DAPI in CA3 area between in PINK1-KO and WT controls. The results are expressed as mean \pm S.E.M. Circles represent individual mean fluorescence signal intensity in one section. Three animals per genotype were used for the analysis. Statistical significance is indicated by $**P < 0.01$, when compared to WT. This figure is reprinted version from the Supplemental Figure 1 of Kataoka, K. *et al.*, 2020¹²⁸.

CA3 pyramidal and DG granule cell layer shows significant reduction in Ser65-pUb expression in PINK1-KO

The hippocampal body is composed of the CA and DG regions. These regions can be further divided into 10 subregions that are anatomically distinct (**Fig. 3.1.2.3A**). These hippocampal subregions play important cooperative or uncooperative roles in memory and learning. To test which subregion(s) shows significant alteration in Ser65-pUb expression by PINK1 deficiency, the density of Ser65-pUb-positive cells in each hippocampal subregion was examined in PINK1-KO and WT controls. In PINK1-KO, Ser65-pUb-positive cells were detected especially in the CA1/3 oriens and pyramidal cell layers, DG granule cell layer, and hilus and, to a lesser extent, in the CA3 radiatum and stratum lacunosum moleculare (**Fig. 3.1.2.3B**). The CA1 radiatum and DG molecular layer exhibited almost no Ser65-pUb-positive cells (**Fig. Fig. 3.1.2.3B**). Notably, in PINK1-KO, the density of Ser65-pUb-positive cells was significantly decreased in the CA3 pyramidal cell layer and DG granule cell layer (**Fig. 3.1.2.3B**). These results indicate that PINK1 deletion affects Ser65-pUb expression in specific hippocampal subregions; CA3 pyramidal cell layer and DG granule cell layer.

A



1. CA1 oriens
2. CA1 pyramidal
3. CA1 radiatum
4. CA3 oriens
5. CA3 pyramidal
6. CA3 radiatum
7. Stratum lacunosum moleculare
8. DG granule
9. DG molecular
10. Hilus

B

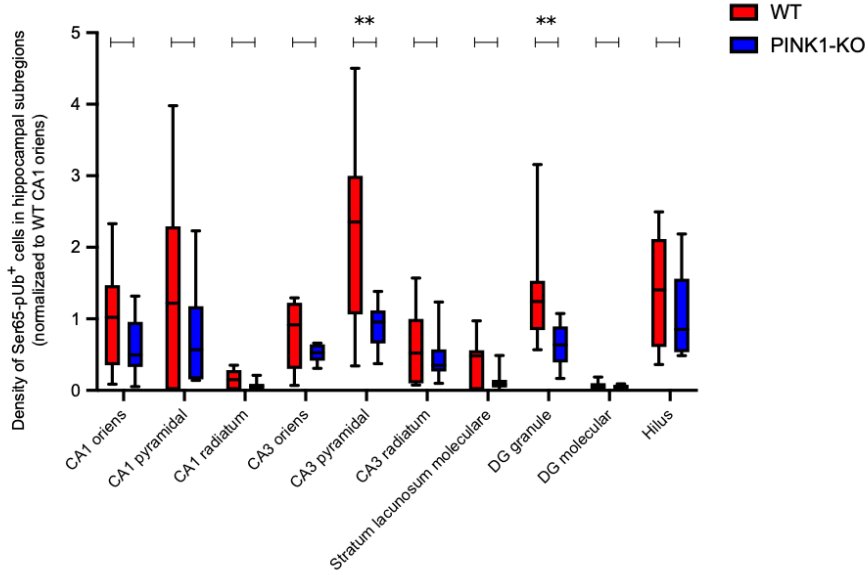


Fig. 3.1.2.3. CA3 pyramidal cell layer and DG granule cell layer show the most significant reduction in the density of Ser65-pUb-positive cells in PINK1-KO. (A) Ten subregions in hippocampus are shown based on anatomical characteristics from DAPI and Ser65-pUb images. (B) Quantitative analysis on the density of Ser65-pUb-positive cells in the indicated hippocampal subregions. PINK1-KO showed reduction in the density of Ser65-pUb-positive cells in CA3 pyramidal cell layer and DG granule cell layer. The box plots represent minimum to maximum values, with the box denoting the 25th, 50th (median), and 75th percentile. Three animals per genotype were used for the analysis. Statistical significance is indicated by $**P < 0.01$, when compared to WT. This figure is reprinted version from the Figure 1C and Supplemental Figure 2A of Kataoka, K. *et al.*, 2020¹²⁸.

Staining specificity of Ser65-pUb antibody in mouse hippocampus

As the animals used in this experiment were approximately 7 months old, lipofuscin autofluorescence might affect interpretation of Ser65-pUb immunoreactivity. Thus, localization of lipofuscin and Ser65-pUb signal was investigated. As a result, lipofuscin autofluorescence signal was distinguishable from Ser65-pUb fluorescence signal (**Fig. 3.1.2.4A**). In addition, the nuclei of cells in the CA1/3 pyramidal cell layers were also immunoreactive against Ser65-pUb in both PINK1-KO and WT controls (**Fig. 3.1.2.4B**). However, no differences were detected between the two genotypes regarding Ser65-pUb signal intensities in DAPI-positive areas (**Fig. 3.1.2.4B**), indicating that the immunoreactivity observed in nuclei in CA1/3 pyramidal cell layers might be unspecific. These results suggest that high levels of Ser65-pUb signal that are observed in a subset of cells in hippocampus may not be due to an unspecific staining of antibody.

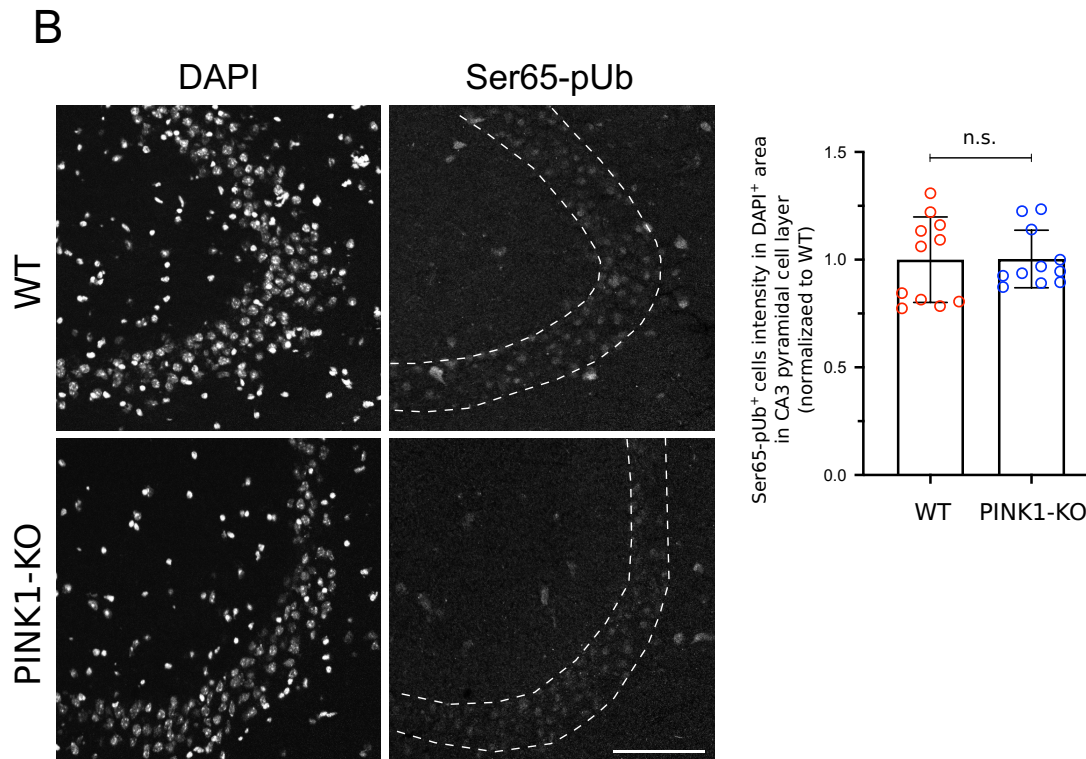
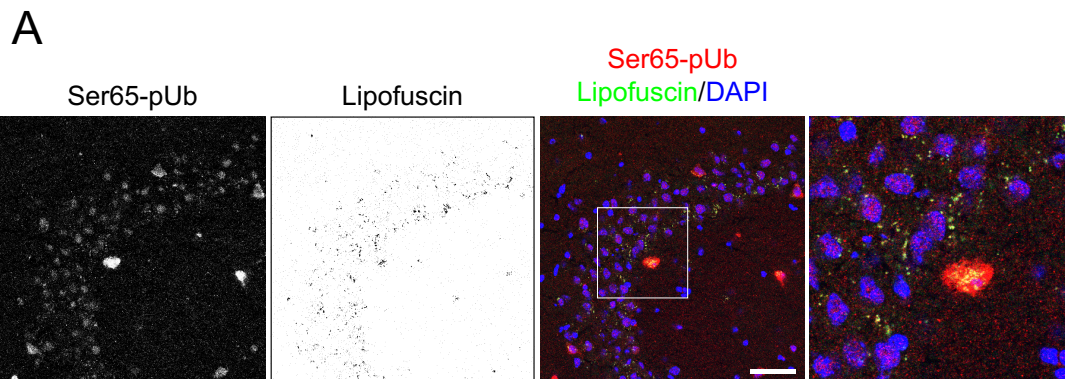
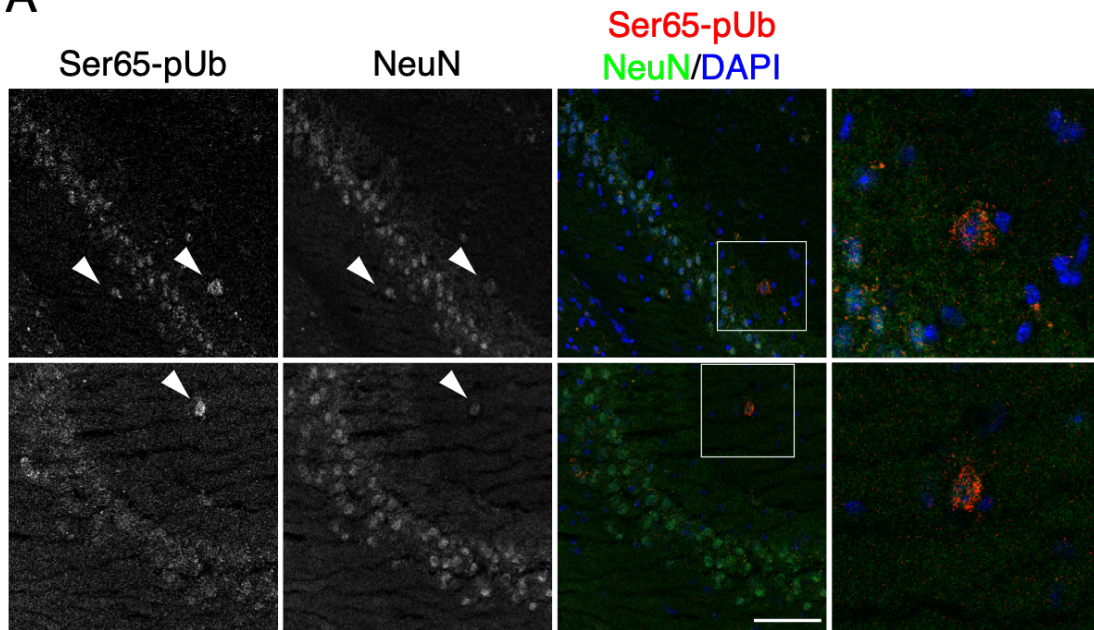


Fig. 3.1.2.4. The strong signal of Ser65-pUb in a subset of the cells in hippocampus may not be due to unspecific staining. (A) Representative confocal microscopy images of hippocampal CA3 region. Coronal sections were immunostained with anti-Ser65-pUb (red). Lipofuscin autofluorescence signal was obtained by acquiring the overlapping pixels of emission at 510-530 nm (green) and at 570-600 nm (red) with excitation at 488 nm and 561 nm, respectively. Nucleus was stained with DAPI (blue). Boxed regions are shown magnified on the right. Scale bar indicates a length of 20 μm . (B) Representative confocal microscopy images of hippocampal CA3 regions in PINK1-KO and WT controls. Coronal sections were immunostained with Ser65-pUb antibody. Nucleus was stained with DAPI. Dotted line surrounds CA3 pyramidal cell layer. Scale bar indicates a length of 100 μm . Shown is quantitative analysis on Ser65-pUb fluorescence signal intensity in DAPI-positive area of CA3 pyramidal cell layer from PINK1-KO and WT controls. Results are expressed as mean \pm S.E.M. Circles represent means signal intensity from one section. Three animals per genotype were used for the analysis. n.s. indicates not significant. This figure is reprinted version from the Supplemental Figures 3 and 4 of Kataoka, K. *et al.*, 2020¹²⁸.

Ser65-pUb-positive cells express neuronal markers

The brain comprises neurons as well as glial cells, such as astrocytes. Thus, the type of hippocampal cells that express Ser65-pUb was next examined. Ser65-pUb signal was expressed predominantly in cells expressing neuronal marker (NeuN) (**Fig. 3.1.2.5A**), and not in astrocytic marker (GFAP) (**Fig. 3.1.2.5B**), in the hippocampus. These results indicate that, in physiological conditions, hippocampal neurons express Ser65-pUb in a PINK1-dependent manner.

A



B

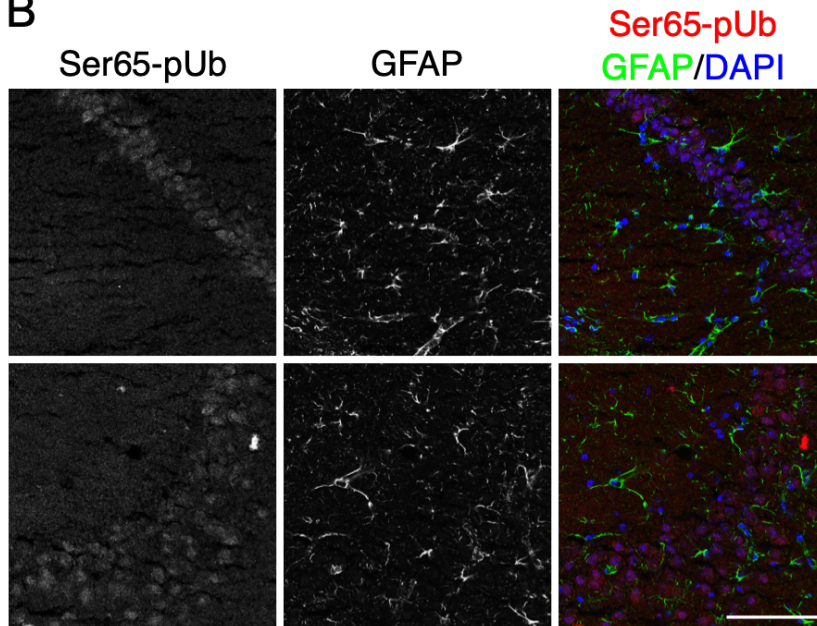


Fig. 3.1.2.5. Ser65-pUb signal co-localizes to neuronal markers, but not to astrocytic markers, in hippocampus. (A) Representative confocal microscopy images of hippocampal CA1 (upper images) and CA3 (lower images) regions. Coronal sections were immunostained with anti-Ser65-pUb (red), and anti-NeuN (green) antibodies. Nuclei were stained with DAPI (blue). The boxed regions are magnified on the right. The white arrows indicate Ser65-pUb-positive cells expressing NeuN. Scale bar indicates a length of 100 μm . (B) Representative confocal microscopy images of hippocampal CA1 (upper images) and CA3 (lower images) regions. Coronal sections were immunostained with anti-Ser65-pUb (red) and anti-GAFP (green) antibodies. Nuclei were stained with DAPI (blue). Scale bar indicates a length of 100 μm . This figure is reprinted version from the Figure 2 of Kataoka, K. *et al.*, 2020¹²⁸.

3.1.3. Discussion

Ubiquitin phosphorylation at Serine 65 is a key step in the efficient execution of PINK1 and Parkin-dependent mitophagy¹⁰⁵. The physiological and pathological importance of ubiquitin phosphorylation has been suggested in the previous studies^{121–123}. However, immunohistochemical data on ubiquitin phosphorylation are missing in mouse models, that the *in situ* information on ubiquitin phosphorylation in tissues is still scarce. In this section, the immunohistochemical characteristics of Ser65-pUb was investigated in the mouse hippocampus.

PINK1-mediated formation of Ser65-pUb may be important for preserving integrity of hippocampal neuron

Some cells expressed Ser65-pUb strongly throughout the hippocampus, while other cells expressed no or low levels of Ser65-pUb (**Fig. 3.1.2.1**). These Ser65-pUb-positive cells were significantly decreased in PINK1-KO, indicating that PINK1 might be physiologically active in the hippocampus (**Fig. 3.1.2.1**). Furthermore, the CA3 pyramidal and DG granule cell layer showed the most significant reduction in the density of Ser65-pUb-positive cells in PINK1-KO hippocampus (**Fig. 3.1.2.3**). A morphometric analysis of the subcortical gray structure in Parkinson's disease (PD) patients showed that the CA3 and DG exhibit serious atrophy^{129,130}, raising the possibility that PINK1-mediated Ser65-pUb formation is important for a proper structure and function of the hippocampus in the context of PD. Moreover, Ser65-pUb was mainly expressed in cells with neuronal markers (**Fig. 3.1.2.5**). This is consistent with previous studies using *in situ* hybridization technique that shows the

PINK1 mRNA is strongly expressed in neurons, particularly in the hippocampal CA3 layer, with little to no expression in glial cells in the rodent brain^{131,132}. Of note, mitophagy is important for proper neuronal function and survival via the maintenance of a healthy pool of mitochondria^{133,134}. Thus, Ser65-pUb might play an important role in preserving neurons in the mouse hippocampus through mitophagy.

Possibility of PINK1-independent generation of Ser65-pUb

PINK1 is the only known kinase that can phosphorylate ubiquitin at Serine 65. However, PINK1 deficiency resulted in a significant reduction in the density of Ser65-pUb-positive cells, while several Ser65-pUb-positive cells were still detected in the hippocampus of PINK1-KO (**Fig. 3.1.2.1**). In *Drosophila* model lacking *PINK1* gene homolog, PINK1-independent Ser65-pUb signals were also detected in regions adjacent to the PPM2 cluster¹²¹. These findings suggest that one or more uncharacterized kinases other than PINK1 have a potential to generate Ser65-pUb. However, there is the possibility that this PINK1-independent fluorescence signal results from unspecific staining.

Decreased expression in Ser65-pUb may be not due to reduction in neuronal number

One may argue that the decreased density of Ser65-pUn-positive cells may not result from PINK1 deficiency; rather, it may be attributed to a reduction in neuronal density. However, the data in this study shows that DAPI signal intensities were comparable between PINK1-KO and WT control (**Fig. 3.1.2.2**), indicating that the total number of cells in hippocampus were not affected by the

genotype. Loss of PINK1 was previously shown to impede the differentiation of neuronal stem cells through mitochondrial defects in the DG subgranular zone of the hippocampus¹³⁵. Nevertheless, the same study demonstrated that neuronal density in the hippocampus is unchanged in PINK1-deficient mice¹³⁵. In addition, several studies have suggested that PINK1-KO do not show neurodegeneration, despite pronounced mitochondrial dysfunction⁵⁰. These studies support reduction in the density of Ser65-pUb-positive cells in PINK1-KO may be due to defect in PINK1 activity in neurons, rather than a reduction in density of neurons.

3.1.4. Conclusion

From the obtained results, Ser65-pUb may be useful for biomarker of *in situ* PINK1 activity in the mouse hippocampus. However, these results should be interpreted with cautions, as a substantial number of Ser65-pUb-positive cells was observed even in the absence of PINK1. This indicates that uncharacterized kinase(s) might regulate the expression of Ser65-pUb. As PINK1 expression is prevalent not only in the brain, but also in peripheral tissues with high metabolic demand (such as the heart), further analyses of Ser65-pUb in different organs of the mouse are warranted.

3.2. Age-dependent dual functions of cannabinoid CB1 receptor in mitochondrial dynamics and autophagy

3.2.1. Introduction

ECS and brain aging

As described in Chapter 1, the ECS is widely distributed in the CNS, constituting a complex signaling system that modulates synaptic transmission and glial activation^{71,136}. Of numerous biological roles of the ECS, accumulating evidence suggests that the ECS in the CNS, especially CB1 receptor, undergoes age-dependent alterations, which influences speed of memory decline in human and rodents (**Fig. 3.2.1.1**). 2-AG level is reduced in brain of older animals¹³⁷. Moreover, gene expression level of CB1 receptor and the coupling of CB1 receptor to G protein are reduced in the specific brain regions including hippocampus with advancing age¹³⁸. CB1 deficient mice (CB1-KO) shows age-dependent acceleration in cognitive decline, which is accompanied by the significant neuronal loss in hippocampal CA1 and CA3 region^{90,103}. In contrast to adult animals, young CB1-KO shows better memory performance than age-matched WT¹³⁹. Further, a chronic low dose THC, the CB1 agonist, treatment abolishes age-dependent memory decline¹⁴⁰. THC treatment in young animals worsens their memory and learning performance, in good agreement with the well-known adverse effects of THC seen in young animals and humans¹⁴¹. Collectively, these studies suggest that CB1 receptor experiences alterations in quantity and quality along the aging, raising the possibility that CB1 activity might be critical for neuronal integrity and memory performance through lifespan. However, the causative link between CB1 receptor and neuronal homeostasis is still unknown.

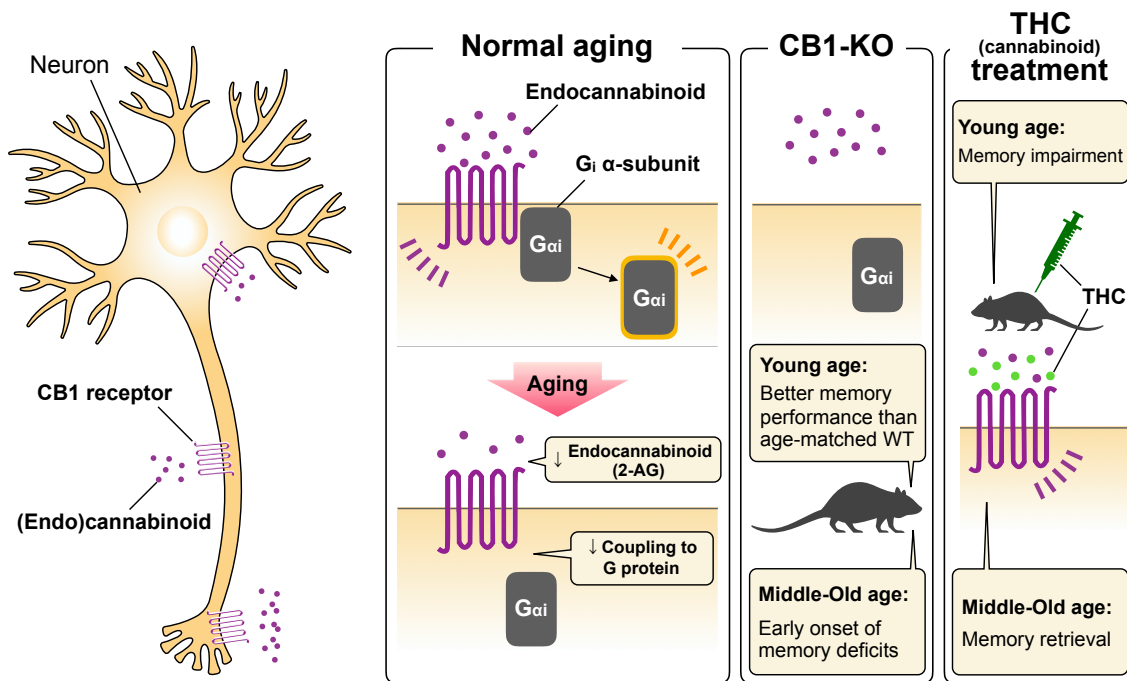


Fig. 3.2.1.1. The ECS and brain aging

Functional modulation of mitochondria by CB1 activity

In Chapter 1, the involvement of CB1 receptor in metabolism was described. As mitochondria are center for cellular metabolism, it is no wonder that metabolic control by CB1 receptor is involved in mitochondria. Indeed, emerging evidence has recently linked CB1 receptor to mitochondria⁹⁹. Early studies have suggested that THC could impair isolated mitochondrial function in murine brain and skeletal muscle¹⁴². Additionally, anandamide, the major endocannabinoid, has been also reported to inhibit mitochondrial oxidative phosphorylation and ATP synthesis in isolated mitochondria from rat primary decidual cells¹⁴³. Exogenous cannabinoids, like THC and HU210, treatment have a negative impact on mitochondrial respiratory function and membrane potential,

which is accompanied by significant production of mitochondrial ROS including hydrogen peroxide^{144,145}. Moreover, cannabinoid receptor stimulation impairs mitochondrial biogenesis in white adipocytes¹⁴⁶. Mitochondrial morphology is also affected by endocannabinoid, as anandamide treatment causes swelling of isolated mitochondria and decreased membrane potential¹⁴⁷. Conversely, blockade of CB1 receptor by rimonabant increases the mitochondrial biogenesis and function in high fat diet-fed mice⁹⁴. These findings indicate that CB1 receptor seems to be implicated in mitochondrial oxidative capacity, membrane potential, energy production and biogenesis.

Mitochondrial localization of CB1 receptor in mitochondria

Notably, CB1 receptor has been recently found on the mitochondrial outer-membrane in tissues with high energy demand such as hippocampal neuron and striated muscle^{100,148}. Mitochondrial CB1 receptor alters neuronal energy metabolism through intra-mitochondrial cAMP-PKA axis¹⁰¹. Interestingly, memory impairment induced by acute treatment of cannabinoids requires the activation of the mitochondrial CB1 receptor in hippocampus¹⁰¹. These studies suggest that neuronal energy metabolism mediated by mitochondrial CB1 receptor might be crucial for the memory function in hippocampus.

The aim of this section

CB1 receptor might be critical for neuronal integrity to keep memory function through the lifespan. Moreover, recent studies have emphasized on mitochondrial functions of CB1 receptor, and possibly

its implication to metabolic control. Thus, it is possible that CB1 receptor might regulate mitochondrial integrity in hippocampal neurons. In this section, the effect of CB1 deficiency on mitochondrial dynamics such as mitophagy and mitochondrial morphology was investigated. First, Ser65-pUb expression was found to be reduced in adult CB1-KO hippocampus, especially in CA1 pyramidal cell layer. In young animals, Ser65-pUb expression was comparable in CB1-KO and WT controls. Consistently, mitophagy occurred less frequently in hippocampal neuron of adult CB1-KO, while young CB1-KO showed unchanged frequency compared to age-matched young WT controls. Moreover, adult CB1-KO exhibited mitochondrial elongation and interconnection in CA1 hippocampal neurons. These findings suggest that loss of CB1 receptor may lead to age-dependent alterations in mitochondrial dynamics in mouse hippocampus.

3.2.2. Results

Ubiquitin phosphorylation at Serine 65 (Ser65-pUb) is decreased in hippocampus of adult CB1-KO

To investigate whether CB1 deficiency influences mitophagy activity in hippocampus, Ser65-pUb expression in hippocampus of adult CB1-KO and WT controls was investigated. Ser65-pUb is formed by PINK1 activity in mitochondria to induce mitophagy, offering a biomarker for mitophagy^{54,111,127}. As described in Chapter 3.2, a subset of hippocampal cells strongly expresses Ser65-pUb throughout the hippocampus, while the other cells express no or low levels of Ser65-pUb. Moreover, PINK1 deficiency leads to partial reduction in the density of Ser65-pUb-expressing cells. In this study, the density of Ser65-pUb-positive cells was examined in hippocampus of young (1-2 months old) and adult (6-7 months) CB1-KO and WT controls. As expected, these animals showed that a subset of cells in hippocampus expressed strong signal for Ser65-pUb, while the other cells not (**Fig. 3.2.2.1A**). The density of Ser65-pUb-positive cells in hippocampus was not altered in WT across generations (**Fig. 3.2.2.1B**). However, adult CB1-KO showed significant decrease in the density of Ser65-pUb-positive cells in hippocampus along the aging (**Fig. 3.2.2.1B**). Adult CB1-KO also exhibited reduced Ser65-pUb signal compared to age-matched adult WT (**Fig. 3.2.2.1B**). These results suggest that adult CB1-KO show a reduction in mitophagy activity in hippocampus, but not in young mice.

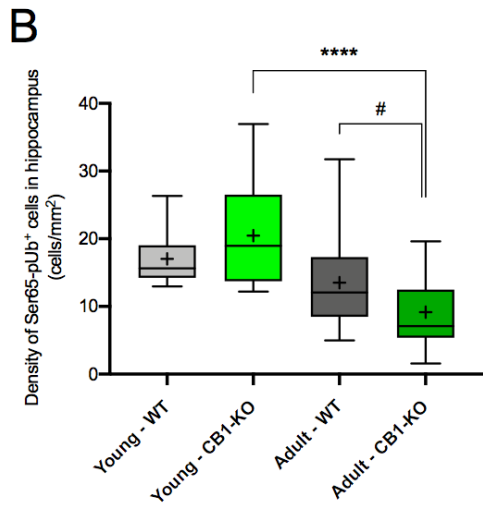
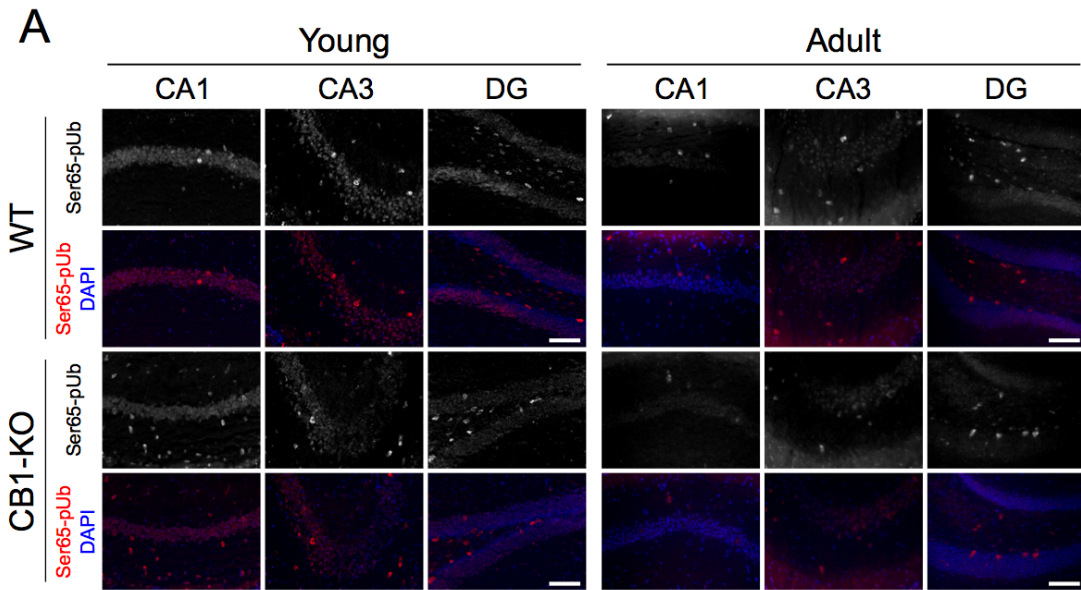


Fig. 3.2.2.1. The density of Ser65-pUb-positive cells was decreased in hippocampus of adult CB1-KO. (A) Representative images of hippocampus (CA1, CA3 and DG) of indicated animals showing Ser65-pUb signal (red) and DAPI (blue). A subset of cells in hippocampus was positive for Ser65-pUb, while the other cells not. Scale bars indicate length of 100 μ m. (B) Quantitative analysis on the density of Ser65-pUb-positive cells in hippocampus. Standard box plots of value in each slice with median (25th and 75th percentiles) and whiskers (at minimum and maximum value) are shown. “+” indicates means. CB1-KO showed the decreased density of Ser65-pUb-positive cells in hippocampus along the aging. Adult CB1-KO showed the reduction in the density of Ser65-pUb-positive cells compared to age-matched adult WT. Young – WT: $n = 17$ slices from $n = 4$ animals, Young – CB1-KO: $n = 17$ slices from $n = 4$ animals, Adult – WT: $n = 25$ slices from $n = 6$ animals, Adult – CB1-KO: $n = 29$ slices from $n = 6$ animals. Statistical significance is indicated by **** $P < 0.0001$ for age effect, and # $P < 0.05$ for genotype effect. This figure is reprinted version from the Figure 1 of Kataoka *et al.*, 2020¹⁴⁹.

CA1 pyramidal cell layer shows significant alteration in Ser65-pUb expression in age-dependent manner

As described in Chapter 3.2, hippocampus can be divided into 10 subregions. Individual subregion has their characteristic expression levels of Ser65-pUb. To examine Ser65-pUb expression of which subregion is affected by CB1 deficiency, the density of Ser65-pUb-positive cells in each hippocampal subregion was checked. In WT controls, the densities of Ser65-pUb-positive cells were unchanged along the aging, except for CA3 radiatum (**Fig. 3.2.2.2**). In adult CB1-KO, the densities of Ser65-pUb-positive cells were significantly decreased in 6 subregions (CA1 oriens, CA1 pyramidal, CA3 pyramidal, CA3 radiatum, Stratum lacunosum moleculare and Hilus) (**Fig. 3.2.2.2**). Of these subregions, CA1 pyramidal cell layer showed interesting pattern of expression change, that the density of Ser65-pUb-positive cells was decreased in CB1-KO compared to age-matched WT in adult generations, whereas this phenomenon was reversed in young generations (**Fig. 3.2.2.2**). These results suggest that CB1 deficiency may significantly influence Ser65-pUb expression particularly in CA1 pyramidal cell layer.

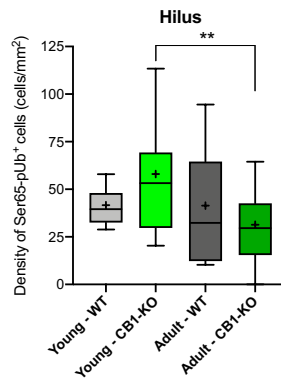
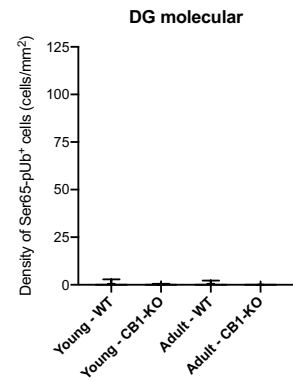
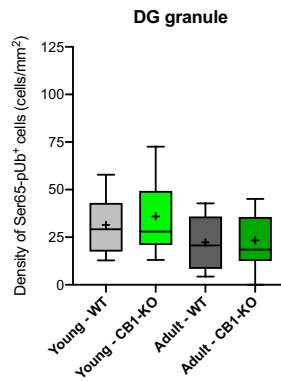
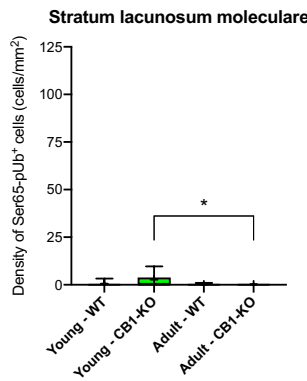
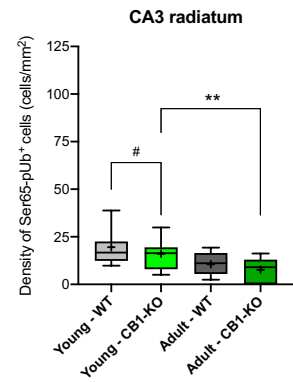
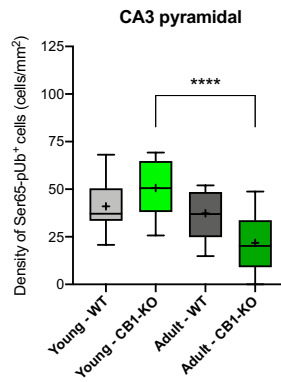
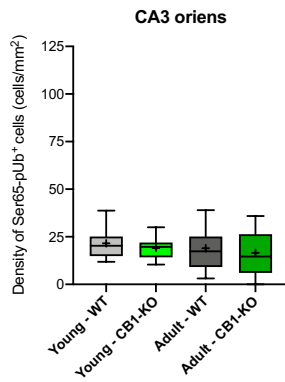
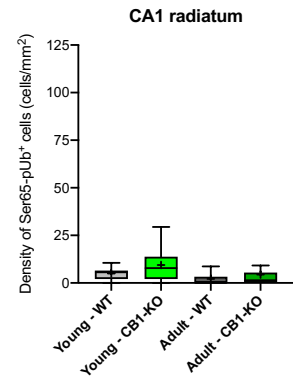
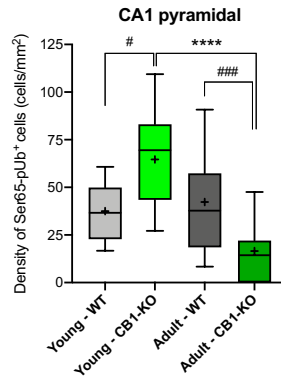
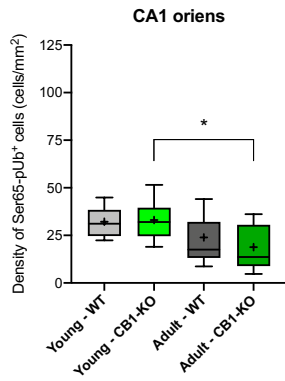
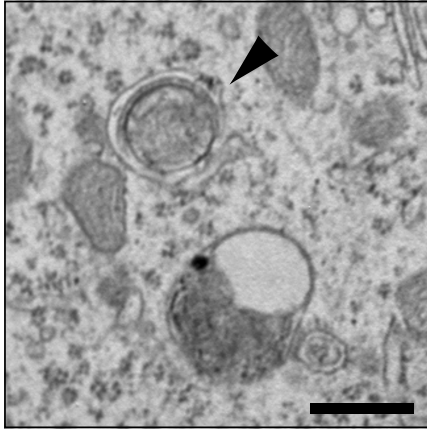


Fig. 3.2.2.2. CB1 deficiency differentially alters the density of Ser65-pUb-positive cells in distinct hippocampal subregions across the generations. Quantitative analysis on the density of Ser65-pUb-positive cells in hippocampal subregions (CA1 oriens, CA1 pyramidal, CA1 radiatum, CA3 oriens, CA3 pyramidal, CA3 radiatum, Stratum lacunosum moleculare, DG granule, DG molecular, Hilus). Standard box plots of value in each slice with median (25th and 75th percentiles) and whiskers (down to 10th and up to 90th percentiles) are shown. “+” indicates mean. Note that in CA1 pyramidal cell layer, the effect of CB1 deficiency on the density of Ser65-pUb was opposite between young and adult age. Young – WT: $n = 17$ slices from $n = 4$ animals, Young – CB1-KO: $n = 17$ slices from $n = 4$ animals, Adult – WT: $n = 25$ slices from $n = 6$ animals, Adult – CB1-KO: $n = 29$ slices from $n = 6$ animals. Statistical significance is indicated by $*P < 0.05$, $**P < 0.01$ and $****P < 0.0001$ for age affect, and $\#P < 0.05$ and $###P < 0.001$ for genotype effect. This figure is reprinted version from the Figure 2 of Kataoka *et al.*, 2020¹⁴⁹.

Mitophagy-like events are less in adult CB1-KO hippocampus

To corroborate the findings above, transmission electron microscope (TEM) was used to observe mitophagy occurring in hippocampal neurons. Mitophagy accompanies with sequestering damaged mitochondria with double-membraned structure (autophagosome) and then fusion with lysosome. In neurons, mitochondria that are destined for mitophagy are delivered from axon and dendrite to neuronal soma¹⁵⁰. Thus, mitochondria that were sequestered by autophagosome-like structures in neuronal soma are defined as mitophagy-like events (**Fig. 3.2.2.3A**). To investigate whether CB1 receptor influence the frequency of mitophagy in hippocampus, the mitophagy-like events in CA1 neuronal soma was counted in a blinded manner. It was found that these events were comparable between young CB1-KO and WT controls (**Fig. 3.2.2.3B**), yet adult CB1-KO exhibited significantly reduced mitophagy-like events compared to age-matched WT controls (**Fig. 3.2.2.3B**). This result verifies that mitophagy activity is reduced in hippocampal CA1 pyramidal neuron of adult CB1-KO.

A



B

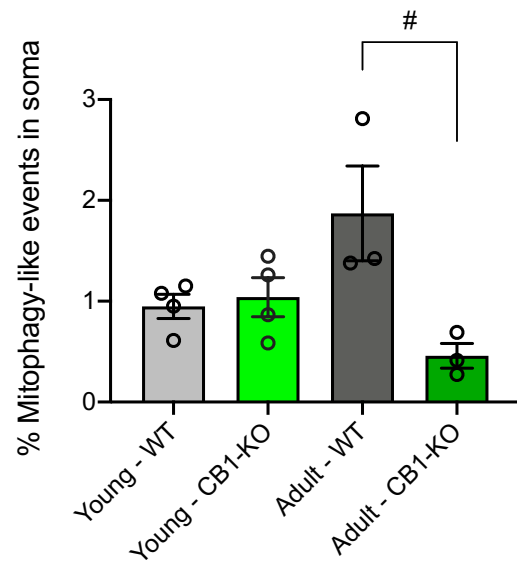


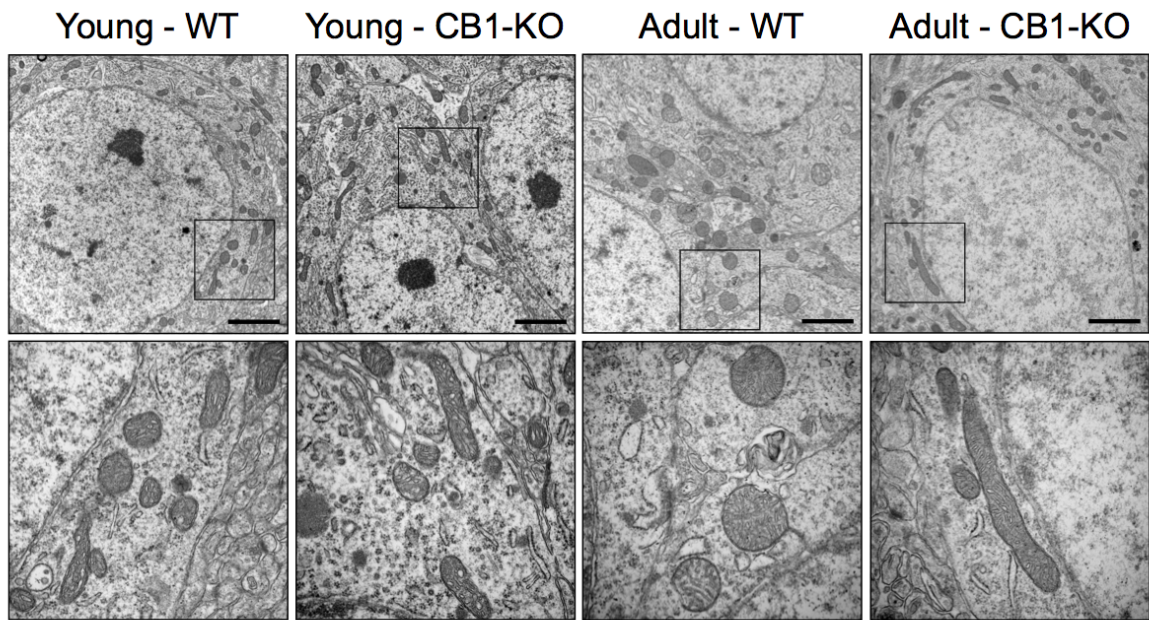
Fig. 3.2.2.3. Mitophagy-like events are reduced in neuronal soma in hippocampal CA1 pyramidal cell layer in CB1-KO. (A) Representative electron micrograph showing mitophagy-like event occurring in neuronal soma in CA1 pyramidal cell layer. Mitochondria that were sequestered by double-membraned structures (autophagosome) are defined as mitophagy-like events. Black arrowhead indicates mitophagy-like event. Scale bar represents 500 nm. (B) Quantitative analysis on the frequency of mitophagy-like events in indicated animal groups. Percentages of mitophagy-like events in the total number of mitochondria were calculated. Mitophagy-like events in adult CB1-KO were less than age-matched WT controls. Circles represent data from individual mice. Data are expressed as means \pm S.E.M. Young – WT: $n = 4$ animals, Young – CB1-KO: $n = 4$ animals, Adult – WT: $n = 3$ animals, Adult – CB1-KO: $n = 3$ animals. Statistical significance is indicated by $\#P < 0.05$ for genotype effect. This figure is reprinted version from the Figure 3 of Kataoka *et al.*, 2020¹⁴⁹.

TEM analysis shows that mitochondrial morphology changes to elongated structure in CA1

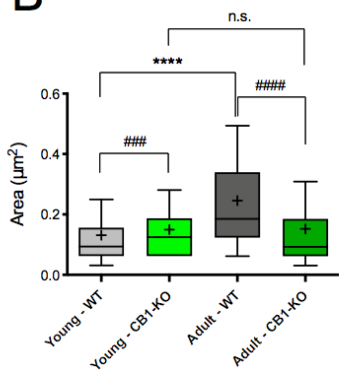
hippocampal neuron of adult CB1-KO

Mitochondrial turnover and function are tightly associated with their morphology⁵⁶. Alterations in mitochondrial morphology have been observed in a wide range of tissues derived from aging-related diseases^{151–155}. To gain insights into the mitochondrial morphology in aged CB1-KO, ultrastructural analysis using TEM was performed to examine mitochondrial morphology in hippocampal CA1 pyramidal neurons. To assess mitochondrial morphology, their area, perimeter and circularity were quantified. As a result, WT showed a significant age-dependent increase in area and perimeter without change in circularity (**Fig. 3.2.2.4**). Heterogeneity of circularity was smaller in adult WT animals compared to young ones, that mitochondrial morphology changed to larger and round shape along the aging (**Fig. 3.2.2.4**). Note that the aging process caused a decrease in mitochondria with low circularity and increase in those with circularity close to 1, as represented by frequency distribution plot of mitochondrial circularity (**Fig. 3.2.2.5**), although the averages between them were comparable. In contrast, CB1-KO animals showed little change in mitochondrial area and perimeter (**Fig. 3.2.2.4**). However, the population of mitochondria with low circularity was significantly increased in CB1-KO significantly as aging (**Fig. 3.2.2.4** and **Fig. 3.2.2.5**), indicating that aged CB1-KO shows mitochondrial elongation. In young generations, area and perimeter were smaller in WT controls than CB1-KO, which was reversed in adult ages (**Fig. 3.2.2.4**). Circularities were comparable between young CB1-KO and WT controls, whereas those of CB1-KO were smaller than WT controls in adult age (**Fig. 3.2.2.4**).

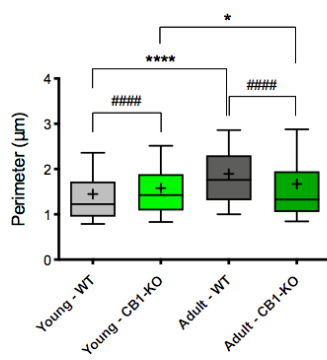
A



B



C



D

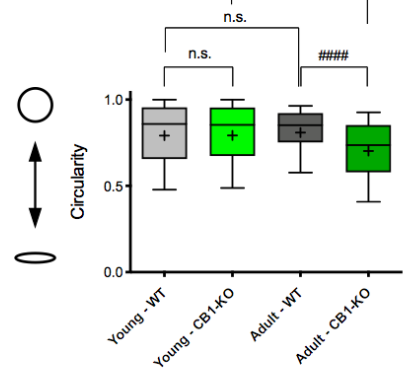


Fig. 3.2.2.4. TEM analysis shows that CB1 deficiency differentially alters mitochondrial morphologies in neuronal soma in hippocampal CA1 pyramidal cell layer along the aging. (A)

Representative electron micrographic images of mitochondria in neuronal soma in hippocampal CA1 pyramidal cell layer. The outlined regions are magnified and shown in the images below. Scale bars represent 2 μm . The results of quantitative analysis on mitochondrial area (B), perimeter (C) and circularity (D) are shown. Standard box plots of each value of individual mitochondria with median (25th and 75th percentiles) and whiskers (down to 10th and up to 90th percentiles) are shown. “+” indicates mean. WT showed the increase in area and perimeter in age-dependent manner, whereas there was no significant change in circularity along the aging. However, CB1-KO showed age-dependent decrease in circularity, while the effects on area and perimeter were limiting. Young – WT: $n = 1,739$ mitochondria from $n = 4$ animals, Young – CB1-KO: $n = 1,488$ mitochondria from $n = 4$ animals, Adult – WT: $n = 1,031$ mitochondria from $n = 3$ animals, Adult – CB1-KO: $n = 1,041$ mitochondria from $n = 3$ animals. Statistical significance is indicated by $*P < 0.05$ and $****P < 0.0001$ for age effect, and $###P < 0.001$ and $#####P < 0.0001$ for genotype effect. n.s. stands for not significant. This figure is reprinted version from the Figure 4 of Kataoka *et al.*, 2020¹⁴⁹.

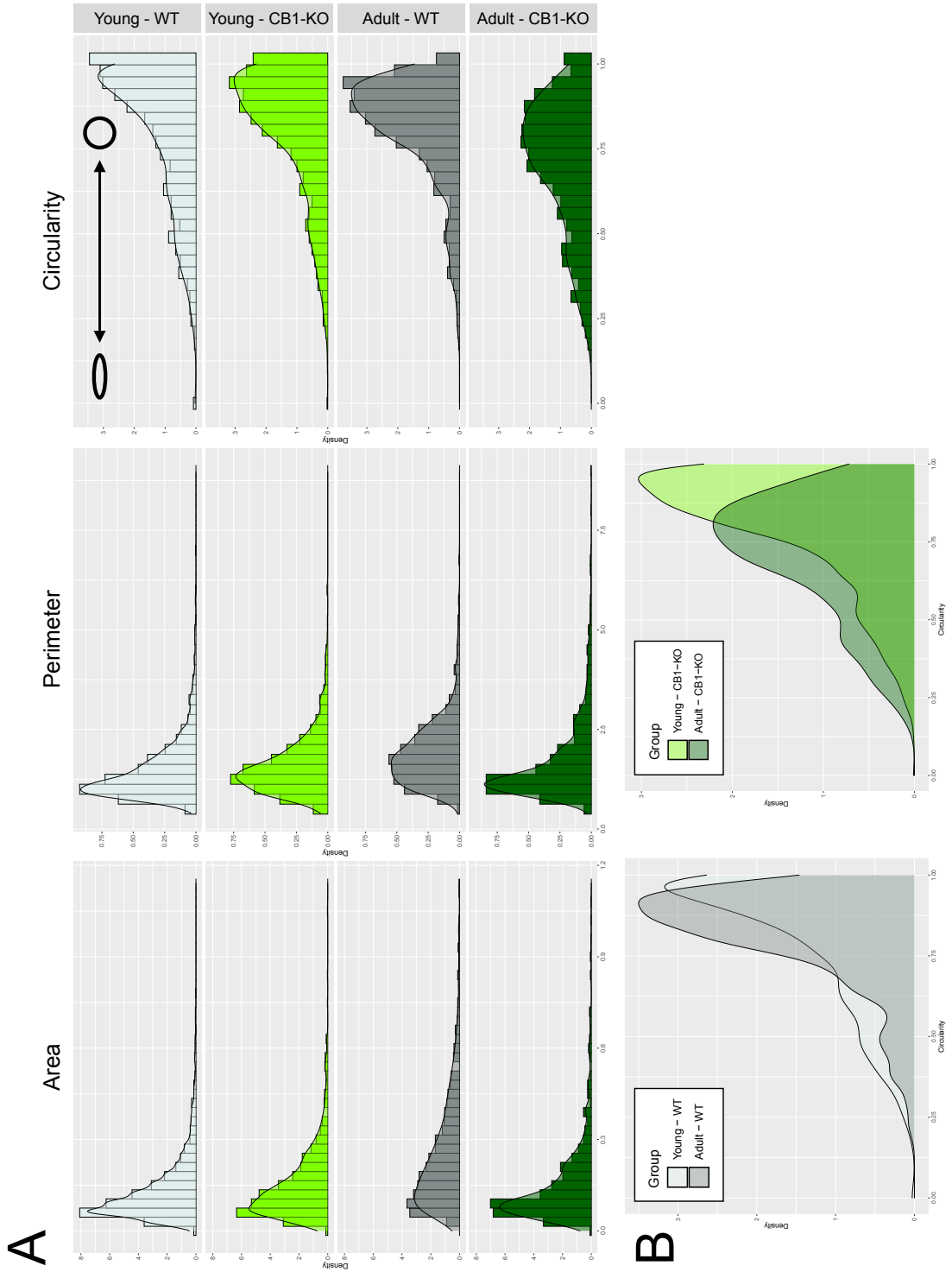


Fig. 3.2.2.5. Frequency distribution of mitochondrial morphology in CB1-KO and WT control across aging. (A) Frequency histogram of mitochondrial area, perimeter and circularity. (B) Overlaid density plot of mitochondrial circularity from (A). Young – WT: $n = 1,739$ mitochondria from $n = 4$ animals, Young – CB1-KO: $n = 1,488$ mitochondria from $n = 4$ animals, Adult – WT: $n = 1,031$ mitochondria from $n = 3$ animals, Adult – CB1-KO: $n = 1,041$ mitochondria from $n = 3$ animals.

FIB/SEM analysis reveals that adult CB1-KO shows mitochondrial elongation and interconnection in hippocampal CA1 neuron

To evaluate the mitochondrial structures more precisely, FIB/SEM was utilized to acquire mitochondrial network organization in single neuronal soma located in CA1 pyramidal cell layer. In young animals of both genotypes, mitochondrial morphology appeared to be comparable (**Fig. 3.2.2.6**). Notably, mitochondrial morphologies in young animals were heterozygous in both genotypes (**Fig. 3.2.2.6**). In contrast, adult WT showed uniform and spherical mitochondria in CA1 cell soma (**Fig. 3.2.2.6**). However, adult CB1-KO showed elongated and interconnected organization (**Fig. 3.2.2.6**). Additionally, individual mitochondria in adult WT sometimes connected with nanotunnel, whereas adult CB1-KO did not show such a structure (**Fig. 3.2.2.6**). This structure is known as “Mitochondria-on-a-string (MOAS)”. MOAS is previously reported to be associated with normal aging and stress-induced disease conditions^{153,156–159}. MOAS is characterized by either free-ended or connecting membrane protrusions across non-adjacent mitochondria in tissues, and thought to be caused by dysfunction in mitochondrial dynamics, in which fission is initiated but incompletely arrested in intermediate step(s)^{153,158}. Overall, present results suggest that adult CB1-KO animals undergo mitochondrial elongation and interconnection in CA1 hippocampal neuronal soma, while WT animals show larger mitochondria with round shape and lose heterogeneity in mitochondrial morphology.

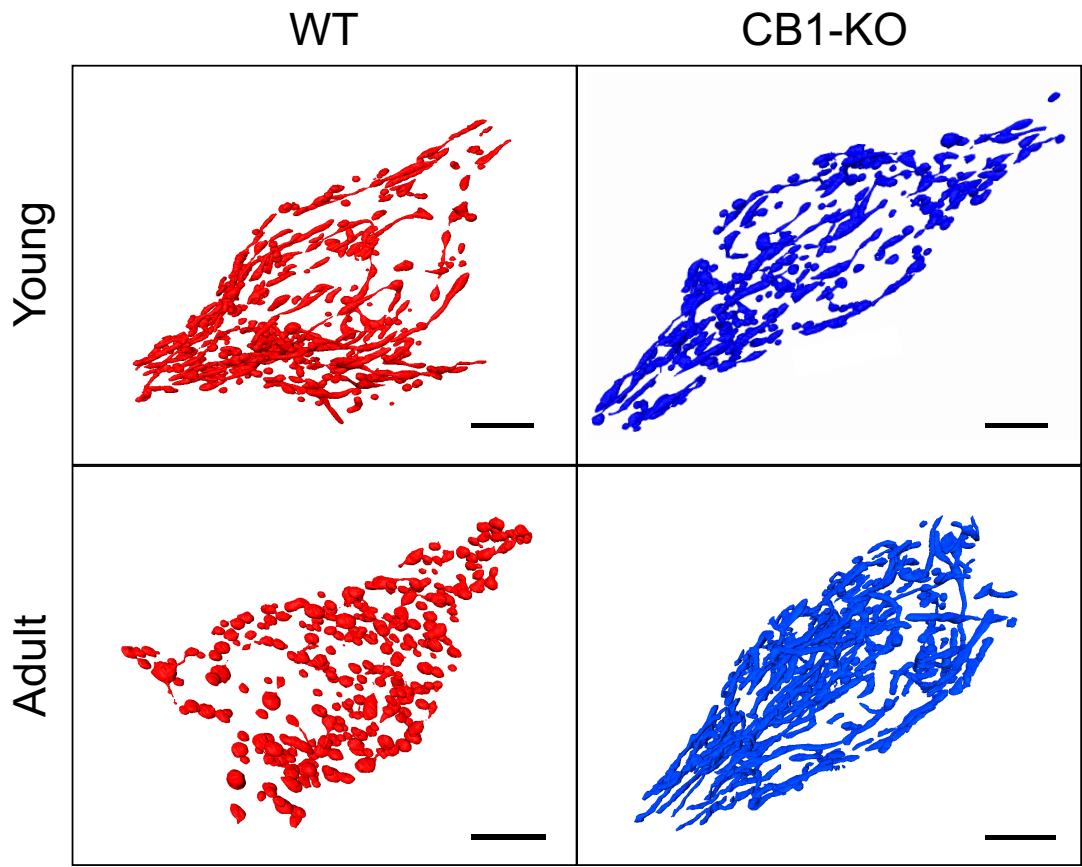


Fig. 3.2.2.6. 3D reconstruction by FIB/SEM revealed that adult CB1-KO shows mitochondrial elongation and interconnection in hippocampal CA1 neuronal soma. Serial cross-sections that included single soma of hippocampal CA1 neuron were obtained by FIB/SEM to reconstruct three-dimensional morphology of mitochondria. Reconstructed mitochondria from young WT (upper left), CB1-KO (upper right), adult WT (lower left) and CB1-KO (lower right) are shown. Mitochondrial morphology appeared to be comparable in young CB1-KO and WT controls. In contrast, mitochondrial pool in adult WT showed uniform, large and round shape, whereas elongated and interconnected mitochondria were found in age-matched adult CB1-KO. Scale bars represent 5 μm . This figure is reprinted version from the Figure 5 of Kataoka *et al.*, 2020¹⁴⁹.

3.2.3. Discussion

Involvement of CB1 receptor in mitophagy

This study showed that the expression of Ser65-pUb in adult CB1 hippocampal neurons was decreased by using immunohistochemical analysis (**Fig. 3.2.2.1**). As Ser65-pUb level correlates with mitophagy flux at least in heart¹²⁷, the decreased level of Ser65-pUb may stem from impaired mitophagy. Consistently, TEM analysis also suggests that mitophagy-like events in CA1 neurons of adult CB1-KO were reduced, compared to those in age-matched WT animals (**Fig. 3.2.2.3**). Decreased mitophagy-like events may be due to either to decreased formation mitochondrial autophagosome or to increased lysosomal activity and/or entity. A previous study has demonstrated that CB1-KO displays a general reduction in lysosomal activity in young and old ages¹⁶⁰. Thus, it may be conceivable that decreased mitochondrial autophagosome formation leads to reduced mitophagy-like events in adult CB1-KO. Mitophagy flux has been reported to decline in hippocampus in aging healthy mice⁴⁵. Because CB1 activity and its ligand level also decrease in hippocampus in age-dependent manner^{137,138}, it is possible that inactivation of CB1 receptor in hippocampus along the aging may contribute to mitophagy defect and non-pathological aging-related memory decline. It would be also noteworthy that mitophagy-like events were comparable in young CB1-KO and WT controls (**Fig. 3.2.2.3**), while young CB1-KO showed a higher density of Ser65-pUb positive cells in CA1 pyramidal cell layer as compared to WT (**Fig. 3.2.2.2**). This discrepancy may be due to the reduction in lysosomal activity in both young and old CB1-KO¹⁶⁰, which can result in transient accumulation of Ser65-pUb level.

Mechanistic insight into CB1 receptor-mediated ubiquitin phosphorylation

In the previous section, it was shown that the density of Ser65-pUb-expressing cells was reduced in hippocampus of PINK1-KO (**Fig. 3.1.2.1**). Notably, basal level of mitophagy *in vivo* is still active even in the absence of PINK1¹²⁴. Thus, it is hypothesized that PINK1-independent ubiquitin phosphorylation could occur in the downstream of CB1 receptor in hippocampus. In immunohistochemical study using *Drosophila* lacking *PINK1* gene homolog, PINK1-independent Ser65-pUb signal is found in some regions in brain¹²¹. It is not known, which kinase is responsible for the PINK1-independent formation of Ser65-pUb, but it was described that protein kinase B (PKB/AKT) regulates mitophagy^{161,162}. In the mouse hippocampus, CB1 receptor activation leads to the phosphorylation of AKT¹⁶³, therefore altered PKB/AKT activity could be a mechanism by which CB1 receptors influenced ubiquitin phosphorylation in this study. Alternatively, because CB1 receptors are G_i coupled they influence protein kinase A (PKA) and thus I κ B kinase (IKK) α activity through the regulation of cAMP levels¹⁶⁴. Activated IKK α phosphorylates next the AMBRA1, which is a regulator of mitophagy in both PINK1/Parkin-dependent and -independent pathways^{165,166}. AMBRA1 mediates the translocation of E3 ubiquitin ligase HUWE1, a key inducing factor in AMBRA1-mediated mitophagy, from cytosol to mitochondria and facilitates the binding of the damaged mitochondria to lysosomes through the LC3/GABARAP complex¹⁶⁵. Further experiments have to clear which mechanism plays a major role in CB1 receptor-mediated ubiquitin phosphorylation and mitophagy.

Mechanistic insight into CB1 receptor-mediated regulation of mitochondrial dynamics

In WT animals, large amount of mitochondrial population in hippocampal neurons showed more rounded shape in the course of aging, as represented by the frequency distribution plot of mitochondrial circularity (**Fig. 3.2.2.4-3.2.2.6**). In contrast, adult CB1-KO showed mitochondrial elongation and interconnection in hippocampal CA1 neurons (**Fig. 3.2.2.4-3.2.2.6**). Mitochondria continuously change their shape through well-coordinated fission and fusion processes, optimizing their bioenergetic capacity⁵⁶. The TEM analysis suggests that mitochondria in adult hippocampal neurons of CB1-KO undergo fusion rather than fission, as adult CB1-KO showed less circularity and more interconnection with advancing aging. A possible downstream molecule of CB1 receptor may be dynamin-related protein 1 (Drp1), known as a fission promoter. Drp1 deletion leads to swollen mitochondria in neurons, redistribution of mitochondria from axon to soma, and age-dependent synaptic defects in hippocampal neurons^{152,167}. Drp1 is functionally regulated by reversible phosphorylation events at multiple residues^{168,169}. For instance, phosphorylation of Drp1 at Ser637 and Ser616 by PKA are associated with inhibition of mitochondrial fission, which leads to increase in elongated mitochondria^{168,169}. Consistently, a previous study suggests that activation of CB1 receptor promotes mitochondrial fission by modulating phosphorylation of Drp1 on both Ser637 and Ser616 residues in renal proximal tubular cells, which are known as metabolically active cells¹⁷⁰. Interestingly, the resulting mitochondrial elongation protects mitochondria from autophagosomal degradation^{65,171}. While mitochondrial morphology itself is not determinant of mitophagy activity¹⁷², fission and fusion process are important for efficient mitophagy, as inhibition of fission or promotion

of fusion weakens mitophagic process⁵⁸. Drp1 is also shown to be recruited to Parkin to trigger fission of mitochondrial subdomain⁶². Thus, it is also probable that CB1 receptor-dependent ubiquitin phosphorylation and subsequent recruitment of Parkin to mitochondria might drive mitochondrial fission.

Involvement of mitochondrially expressed CB1 receptor

Recently, CB1 receptor has been reported to be localized to mitochondrial outer-membrane, not only to cytoplasmic membrane^{100,101}. Interestingly, mitochondrial CB1 is sufficient for causing acute memory impairment induced by high dose of cannabinoids treatment^{100,101}. This effect is mediated, at least partly, through soluble adenylyl cyclase-cAMP-PKA axis which occurs within mitochondria in hippocampus¹⁰¹. PKA is present in various subcellular compartments including mitochondria, and influences the development of diverse physiological and pathological conditions. A number of studies demonstrate that PKA may function in different compartments of mitochondria, and that PKA-dependent phosphorylation of proteins plays an important role in mitochondrial homeostasis¹⁷³. Notably, mitochondrial PKA regulates PINK1 stability in mitochondria and Parkin recruitment to damaged mitochondria¹⁷⁴. These previous studies indicate that mitochondrial CB1 receptor-mediated modulation of PKA activity might underlie altered mitochondrial morphology and even mitophagy in hippocampal neurons.

Age-dependency of CB1 deficiency

Interestingly, the effects of CB1 deletion on mitophagy and mitochondrial morphology were opposite between young and adult animals. This phenomenon resembles that of the previous studies, in which memory and learning in CB1-KO rapidly decreases with advancing age, while in young ages, they perform cognitive tasks even better than age-matched WT controls¹⁷⁵. Furthermore, CB1 agonist THC reverses age-dependent memory deficits, yet these THC effects are abolished in CB1-KO¹⁴⁰. Overall, these findings suggest that CB1 receptor may have differential effects on cellular, physiological and behavioral events in the CNS depending on the age of animals.

3.2.4. Conclusion

In summary, the study in this section suggests that CB1 receptor has age-dependent roles in mitochondrial dynamics in hippocampal neuron, and also strengthens the age-dependency of biological consequences in CB1-KO animals. In adult animals, CB1-KO showed reduced Ser65-pUb and mitophagy, and mitochondrial elongation and interconnection in hippocampal neurons (**Fig. 3.2.4.1**). Accumulating evidence suggest that CB1 receptor organizes different signaling depending on the animals' age. Further studies on the age-dependent functional transition of CB1 receptor are now needed.

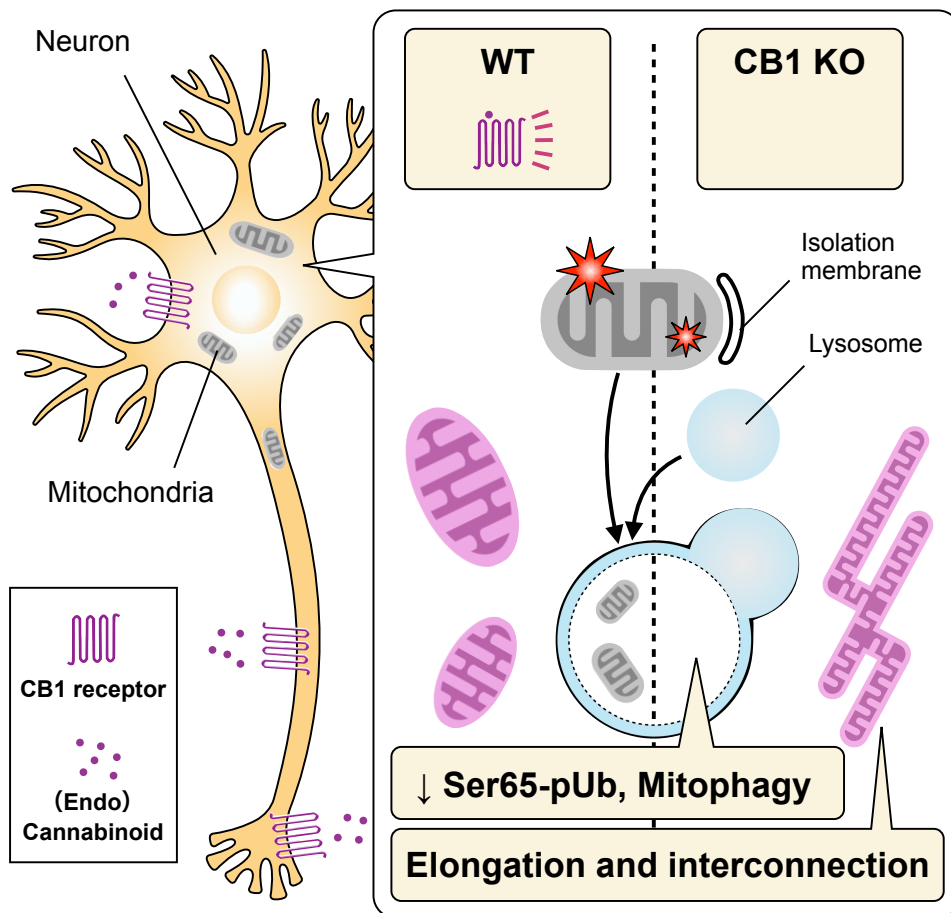


Fig. 3.2.4.1. CB1 deficiency leads to reduced Ser65-pUb, decreased frequency of mitophagy, and mitochondrial elongation and interconnection in adult hippocampal pyramidal neuron.

Chapter 4. Conclusion and Future Prospect

In this thesis, the roles of CB1 receptor in mitochondrial quality control in the mouse hippocampus were described. In Chapter 3.1, the validity of Ser65-pUb immunohistochemistry for measuring hippocampal mitophagy activity was described. In Chapter 3.2, age-dependency of CB1 deficiency in mitophagy and mitochondrial morphology was demonstrated. These studies indicate that CB1 receptor promotes mitophagy and mitochondrial fission, rather than fusion, in hippocampus in age-dependent manner. As mitochondria are the center of bioenergetic processes, especially in tissues with high energy demand, e.g. brain and heart, the role of CB1 receptor in energy homeostasis has to be addressed in the future study. For example, ATP content and mitochondrial membrane potential are the good readouts for energetics in the cell.

This thesis might explain the intriguing phenotype of CB1-KO; that is, young CB1-KO shows superior memory performance but rapidly loses its learning ability in the adult stage. Mitochondria play indispensable roles in generating ATP and calcium homeostasis in brain, both of which are critical for proper neuronal functions such as synaptic vesicle recruitment, synaptogenesis and protein phosphorylation reactions¹⁷⁶. Thus, large amounts of functional mitochondria in neurons possibly contribute to sufficient energy supply and be beneficial for memory performance. In agreement with this, previous *in vitro* studies suggest that reduction in dendritic mitochondrial contents in neurons through enhanced mitophagy leads to defects in dendritic formation^{177,178}, indicating that sufficient amounts of mitochondria might be important for memory formation. As mitochondrial content is determined by the balance between mitochondrial biogenesis and autophagy,

defective mitophagy in CB1-KO can lead to increase in mitochondrial content. Interestingly, as described in the Chapter 3.2, TEM analysis showed that mitochondrial area and perimeter of mitochondria in young CB1-KO were slightly larger than those of age-matched young WT. Although more detailed experiments are needed, these results indicate that young CB1-KO possibly possesses more amounts of mitochondria than age-matched WT as a result of mitophagy defect. Additionally, defect in mitochondrial fission might also contribute to the accumulation of damaged mitochondria. However, mitophagy is essential for maintaining the population of healthy mitochondria. Thus, mitophagy defect in CB1-KO can lead to the rapid accumulation of damaged and/or dysfunctional mitochondria in neurons. The resulting perturbation in energy homeostasis causes memory deficit, as observed in the previous study¹⁰¹.

As mitochondria are the center of energy homeostasis, CB1 receptor is thought to regulate the balance between anabolic and catabolic state through the regulation of mitochondrial dynamics and autophagy. According to the results of this thesis, when CB1 receptor is activated, anabolic state might dominate over catabolic state. In other words, CB1 receptor promotes the synthesis of complex molecules such as protein and lipid from nutrients by consuming energy (anabolic state, or anabolism), rather than the breakdown of complex molecules to generate energy (catabolic state, or catabolism). A number of previous studies has supported this concept. For example, stimulation of CB1 receptor in adipocytes promotes lipogenesis and fat storage, and inhibit mitochondrial biogenesis⁹⁶. Conversely, CB1 blockade induces fatty acid oxidation and mitochondrial biogenesis⁹⁴. Moreover, in starvation, in which catabolism has to be dominated, mitochondria elongate and escape from

mitophagy to sustain ATP production⁶⁵, which resemble those of adult CB1-KO. Previous study also reports that CB1 receptor modulates mechanistic target of rapamycin (mTOR), a crucial regulator for transition between anabolism and catabolism¹⁷⁹. Interestingly, within the CNS, CB1 receptor activates protein synthesis through mTOR in presynapse, which contributes to memory formation¹⁸⁰. Thus, CB1 receptor may sustain memory function along the aging through upregulation of anabolism. Moreover, recent studies suggest that ribosome can be a target of selective autophagy (so-called ribophagy)¹⁸¹. Ribophagy is tightly regulated by the activity of mTOR¹⁸¹. As ribosome biogenesis is responsible for most of energy consumption in the cell (that is, ribosome biogenesis can be catabolic process)¹⁸², it would be tempting to speculate that CB1 receptor regulates different type of selective autophagy to control cellular bioenergetics by modulating the balance between mitophagy and ribophagy (**Fig. 4.1**). Overall, the concept that CB1 receptor regulates energy homeostasis in the CNS will provide unique mechanistic insights into cognitive aging and drive new hypothesis-driven study.

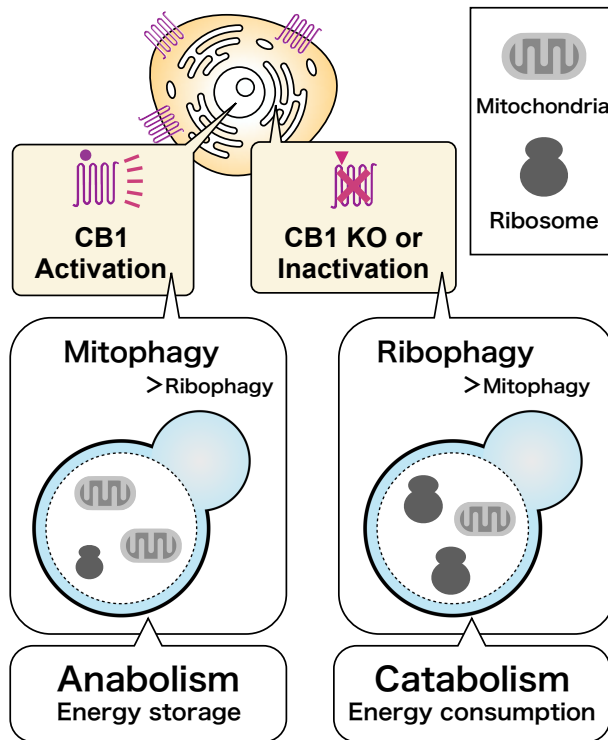


Fig. 4.1. Hypothetical roles of CB1 receptor in different types of selective autophagy

The ECS appears to have evolved as a promoter of energy storage which aims at future use of energy for avoiding starvation⁶⁹. As the ECS, including CB1 receptor, is highly conserved among vertebrates and invertebrate except for insects^{183,184}, it would be interesting to analyze cross-species difference in the speed of brain aging and its involvement of CB1 receptor. For example, *Astyanax mexicanus* is interesting animal model for studying the involvement of CB1 receptor-mediated metabolism in aging. This species consists of river-dwelling and cave-dwelling populations, which experience highly different availability of nutrients; that is, cave-dwelling fish habitat in the cave with poor nutrient source, while river-dwelling ones can easily reach nutrients. Cave-dwelling

fish, but not river-dwelling fish, is known to show high resistance against high glucose-induced senescence¹⁸⁵, indicating that they have a specialized form of metabolism affecting longevity. Interestingly, the brain of cave-dwelling fish shows upregulated gene expression of CB1 receptor, compared to river-dwelling fish¹⁸⁶, which might provide interesting insights into the relationship among CB1 receptor, metabolism and organismal aging. For another example, naked mole rats are the longest-lived rodents which can survive more than 30 years. Interestingly, they do not experience the age-dependent cognitive decline, and their brains are protected from the toxicity of neurodegenerative agents¹⁸⁷. Although it is unknown whether the ECS in naked mole rats has specially evolved, it would be interesting to investigate the mechanism of protection against aging in brain of this species. They seem to possess a gene for CB1 receptor (Gene ID: 101697935). These studies will pave the way for developing therapeutic strategies against a wide range of age-dependent disorders, such as memory decline, in humans, and provide exciting insights into this evolutionally important system.

References

1. López-Otín, C., Blasco, M. A., Partridge, L., Serrano, M. & Kroemer, G. The hallmarks of aging. *Cell* **153**, 1194–1217 (2013).
2. Klass, M. R. A method for the isolation of longevity mutants in the nematode *Caenorhabditis elegans* and initial results. *Mech. Ageing Dev.* **22**, 279–286 (1983).
3. Trifunovic, A. & Larsson, N. G. Mitochondrial dysfunction as a cause of ageing. *J. Intern. Med.* **263**, 167–178 (2008).
4. Park, C. B. & Larsson, N. G. Mitochondrial DNA mutations in disease and aging. *J. Cell Biol.* **193**, 809–818 (2011).
5. Yamano, K., Matsuda, N. & Tanaka, K. The ubiquitin signal and autophagy: an orchestrated dance leading to mitochondrial degradation. *EMBO Rep.* **17**, 300–316 (2016).
6. Harman, D. Aging: a theory based on free radical and radiation chemistry. *J. Gerontol.* **11**, 298–300 (1956).
7. Barja, G. Free radicals and aging. *Trends Neurosci.* **27**, 595–600 (2004).
8. Perez-Campo, R., López-Torres, M., Cadenas, S., Rojas, C. & Barja, G. The rate of free radical production as a determinant of the rate of aging: evidence from the comparative approach. *J. Comp. Physiol. B* **168**, 149–158 (1998).
9. Doonan, R. *et al.* Against the oxidative damage theory of aging: superoxide dismutases protect against oxidative stress but have little or no effect on life span in *Caenorhabditis elegans*. *Genes Dev.* **22**, 3236–3241 (2008).

10. Van Raamsdonk, J. M. & Hekimi, S. Deletion of the mitochondrial superoxide dismutase sod-2 extends lifespan in *Caenorhabditis elegans*. *PLoS Genet.* **5**, e1000361 (2009).
11. Mesquita, A. *et al.* Caloric restriction or catalase inactivation extends yeast chronological lifespan by inducing H₂O₂ and superoxide dismutase activity. *Proc. Natl. Acad. Sci. U. S. A.* **107**, 15123–15128 (2010).
12. Van Remmen, H. *et al.* Life-long reduction in MnSOD activity results in increased DNA damage and higher incidence of cancer but does not accelerate aging. *Physiol. Genomics* **16**, 29–37 (2003).
13. Zhang, Y. *et al.* Mice deficient in both Mn superoxide dismutase and glutathione peroxidase-1 have increased oxidative damage and a greater incidence of pathology but no reduction in longevity. *J. Gerontol. Biol. Sci.* **64**, 1212–1220 (2009).
14. Pérez, V. I. *et al.* The overexpression of major antioxidant enzymes does not extend the lifespan of mice. *Aging Cell* **8**, 73–75 (2009).
15. Trifunovic, A. *et al.* Somatic mtDNA mutations cause aging phenotypes without affecting reactive oxygen species production. *Proc. Natl. Acad. Sci. U. S. A.* **102**, 17993–17998 (2005).
16. Trifunovic, A. *et al.* Premature ageing in mice expressing defective mitochondrial DNA polymerase. *Nature* **429**, 417–423 (2004).
17. Kujoth, G. C. *et al.* Mitochondrial DNA mutations, oxidative stress, and apoptosis in mammalian aging. *Science (80-.).* **481**, 481–484 (2005).

18. Yee, C., Yang, W. & Hekimi, S. The intrinsic apoptosis pathway mediates the pro-longevity response to mitochondrial ROS in *C. elegans*. *Cell* **157**, 897–909 (2014).
19. Rossignol, R. *et al.* Mitochondrial threshold effects. *Biochem. J.* **370**, 751–762 (2003).
20. Hekimi, S., Lapointe, J. & Wen, Y. Taking a ‘good’ look at free radicals in the aging process. *Trends Cell Biol.* **21**, 569–576 (2011).
21. Linnane, A. W., Marzuki, S., Ozawa, T. & Tanaka, M. Mitochondrial DNA mutations as an important contributor to ageing and degenerative diseases. *Lancet* **1**, 642–645 (1989).
22. Bender, A. *et al.* High levels of mitochondrial DNA deletions in substantia nigra neurons in aging and Parkinson disease. *Nat. Genet.* **38**, 515–517 (2006).
23. Kravtsov, Y. *et al.* Mitochondrial DNA deletions are abundant and cause functional impairment in aged human substantia nigra neurons. *Nat. Genet.* **38**, 518–520 (2006).
24. Michikawa, Y., Mazzucchelli, F., Bresolin, N., Scarlato, G. & Attardi, G. Aging-dependent large accumulation of point mutations in the human mtDNA control region for replication. *Science (80-.).* **286**, 774–779 (1999).
25. Taylor, R. W. *et al.* Mitochondrial DNA mutations in human colonic crypt stem cells. *J. Clin. Invest.* **112**, 1351–1360 (2003).
26. Khrapko, K. *et al.* Cell-by-cell scanning of whole mitochondrial genomes in aged human heart reveals a significant fraction of myocytes with clonally expanded deletions. *Nucleic Acids Res.* **27**, 2434–2441 (1999).
27. Clayton, D. A. Replication of animal mitochondrial DNA. *Cell* **28**, 693–705 (1982).

28. Birky, C. W. The inheritance of genes in mitochondria and chloroplasts: Laws, mechanisms, and models. *Annu. Rev. Genet.* **35**, 125–148 (2001).
29. Larsson, N.-G. Somatic Mitochondrial DNA Mutations in Mammalian Aging. *Annu. Rev. Biochem.* **79**, 683–706 (2010).
30. Aspnes, L. E. *et al.* Caloric restriction reduces fiber loss and mitochondrial abnormalities in aged rat muscle. *FASEB J.* **11**, 573–581 (1997).
31. Cohen, H. Y. *et al.* Calorie restriction promotes mammalian cell survival by inducing the SIRT1 deacetylase. *Science (80-.)*. **305**, 390–392 (2004).
32. Bota, D. A. & Davies, K. J. A. Lon protease preferentially degrades oxidized mitochondrial aconitase by an ATP-stimulated mechanism. *Nat. Cell Biol.* **4**, 674–680 (2002).
33. Lee, C. K., Klopp, R. G., Weindruch, R. & Prolla, T. A. Gene expression profile of aging and its retardation by caloric restriction. *Science (80-.)*. **285**, 1390–1393 (1999).
34. Luce, K. & Osiewacz, H. D. Increasing organismal healthspan by enhancing mitochondrial protein quality control. *Nat. Cell Biol.* **11**, 852–858 (2009).
35. Quirós, P. M., Langer, T. & López-Otín, C. New roles for mitochondrial proteases in health, ageing and disease. *Nat. Rev. Mol. Cell Biol.* **16**, 345–359 (2015).
36. Durieux, J., Wolff, S. & Dillin, A. The cell-non-autonomous nature of electron transport chain-mediated longevity. *Cell* **144**, 79–91 (2011).
37. Lee, S. S. *et al.* A systematic RNAi screen identifies a critical role for mitochondria in *C. elegans* longevity. *Nat. Genet.* **33**, 40–48 (2003).

38. Owusu-Ansah, E., Song, W. & Perrimon, N. Muscle mitohormesis promotes longevity via systemic repression of insulin signaling. *Cell* **155**, 699–712 (2013).
39. Zhao, Q. *et al.* A mitochondrial specific stress response in mammalian cells. *EMBO J.* **21**, 4411–4419 (2002).
40. Bennett, C. F. *et al.* Activation of the mitochondrial unfolded protein response does not predict longevity in *Caenorhabditis elegans*. *Nat. Commun.* **5**, 3483 (2014).
41. Ohsumi, Y. Historical landmarks of autophagy research. *Cell Res.* **24**, 9–23 (2014).
42. Johansen, T. & Lamark, T. Selective autophagy mediated by autophagic adapter proteins. *Autophagy* **7**, 279–296 (2011).
43. Clark, S. L. Cellular differentiation in the kidneys of newborn mice studies with the electron microscope. *J. Biophys. Biochem. Cytol.* **3**, 349–362 (1957).
44. Okamoto, K. Organellophagy: eliminating cellular building blocks via selective autophagy. *J. Cell Biol.* **205**, 435–445 (2014).
45. Sun, N. *et al.* Measuring in vivo mitophagy. *Mol. Cell* **60**, 685–696 (2015).
46. Fang, E. F. *et al.* Mitophagy inhibits amyloid- β and tau pathology and reverses cognitive deficits in models of Alzheimer's disease. *Nat. Neurosci.* **22**, 401–412 (2019).
47. Ryu, D. *et al.* Urolithin A induces mitophagy and prolongs lifespan in *C. elegans* and increases muscle function in rodents. *Nat. Med.* **22**, 879–888 (2016).
48. Kitada, T. *et al.* Mutations in the parkin gene cause autosomal recessive juvenile parkinsonism. *Nature* **169**, 166–169 (1998).

49. Valente, E. M. *et al.* Hereditary early-onset Parkinson's disease caused by mutations in PINK1. *Science (80-.)*. **1158**, 1158–1160 (2004).
50. Dawson, T. M., Ko, H. S. & Dawson, V. L. Genetic animal models of Parkinson's disease. *Neuron* **66**, 646–661 (2010).
51. Greene, J. C. *et al.* Mitochondrial pathology and apoptotic muscle degeneration in *Drosophila parkin* mutants. *Proc. Natl. Acad. Sci. U. S. A.* **100**, 4078–4083 (2003).
52. Rana, A., Rera, M. & Walker, D. W. Parkin overexpression during aging reduces proteotoxicity, alters mitochondrial dynamics, and extends lifespan. *Proc. Natl. Acad. Sci. U. S. A.* **110**, 8638–8643 (2013).
53. Clark, I. E. *et al.* *Drosophila pink1* is required for mitochondrial function and interacts genetically with parkin. *Nature* **441**, 1162–1166 (2006).
54. Pickrell, A. M. *et al.* Endogenous Parkin preserves dopaminergic substantia nigral neurons following mitochondrial DNA mutagenic stress. *Neuron* **87**, 371–382 (2015).
55. Thomas, R. E., Andrews, L. A., Burman, J. L., Lin, W. Y. & Pallanck, L. J. PINK1-Parkin pathway activity is regulated by degradation of PINK1 in the mitochondrial matrix. *PLoS Genet.* **10**, e1004279 (2014).
56. Youle, R. J. & van der Bliek, A. M. Mitochondrial fission, fusion, and stress. *Science (80-.)*. **337**, 1062–1065 (2012).
57. Kalia, R. *et al.* Structural basis of mitochondrial receptor binding and constriction by DRP1. *Nature* **558**, 401–405 (2018).

58. Twig, G. *et al.* Fission and selective fusion govern mitochondrial segregation and elimination by autophagy. *EMBO J.* **27**, 433–446 (2008).
59. Egan, D. F. *et al.* Phosphorylation of ULK1 (hATG1) by AMP-activated protein kinase connects energy sensing to mitophagy. *Science (80-.).* **331**, 456–461 (2011).
60. Komatsu, M. *et al.* Impairment of starvation-induced and constitutive autophagy in Atg7-deficient mice. *J. Cell Biol.* **169**, 425–434 (2005).
61. Yamashita, S. I. *et al.* Mitochondrial division occurs concurrently with autophagosome formation but independently of Drp1 during mitophagy. *J. Cell Biol.* **215**, 649–665 (2016).
62. Burman, J. L. *et al.* Mitochondrial fission facilitates the selective mitophagy of protein aggregates. *J. Cell Biol.* **216**, 3231–3247 (2017).
63. James, D. I. & Martinou, J. C. Mitochondrial dynamics and apoptosis: a painful separation. *Dev. Cell* **15**, 341–343 (2008).
64. Tondera, D. *et al.* SLP-2 is required for stress-induced mitochondrial hyperfusion. *EMBO J.* **28**, 1589–1600 (2009).
65. Gomes, L. C., Benedetto, G. Di & Scorrano, L. During autophagy mitochondria elongate, are spared from degradation and sustain cell viability. *Nat. Cell Biol.* **13**, 589–598 (2011).
66. Yoon, Y. *et al.* Formation of elongated giant mitochondria in DFO-Induced cellular senescence : involvement of enhanced fusion process through modulation of Fis1. *J. Cell. Physiol.* **480**, 468–480 (2006).

67. Lee, S. *et al.* Mitochondrial fission and fusion mediators, hFis1 and OPA1, modulate cellular senescence. *J. Biol. Chem.* **282**, 22977–22983 (2007).
68. Lutz, B., Marsicano, G., Maldonado, R. & Hillard, C. J. The endocannabinoid system in guarding against fear, anxiety and stress. *Nat. Rev. Neurosci.* **16**, 705–718 (2015).
69. Piazza, P. V., Cota, D. & Marsicano, G. The CB1 receptor as the cornerstone of exostasis. *Neuron* **93**, 1252–1274 (2017).
70. Di Marzo, V. New approaches and challenges to targeting the endocannabinoid system. *Nat. Rev. Drug Discov.* **17**, 623–639 (2018).
71. Di Marzo, V., Stella, N. & Zimmer, A. Endocannabinoid signalling and the deteriorating brain. *Nat. Rev. Neurosci.* **16**, 30–42 (2015).
72. Atakan, Z. Cannabis, a complex plant: different compounds and different effects on individuals. *Ther. Adv. Psychopharmacol.* **2**, 241–254 (2012).
73. Hayakawa, K. *et al.* Cannabidiol potentiates pharmacological effects of Δ^9 -tetrahydrocannabinol via CB1 receptor-dependent mechanism. *Brain Res.* **1188**, 157–164 (2008).
74. Okamoto, Y., Morishita, J., Tsuboi, K., Tonai, T. & Ueda, N. Molecular characterization of a phospholipase D generating anandamide and its congeners. *J. Biol. Chem.* **279**, 5298–5305 (2004).
75. Bisogno, T. *et al.* Cloning of the first sn1-DAG lipases points to the spatial and temporal regulation of endocannabinoid signaling in the brain. *J. Cell Biol.* **163**, 463–468 (2003).

76. De Petrocellis, L., Nabissi, M., Santoni, G. & Ligresti, A. *Actions and Regulation of Ionotropic Cannabinoid Receptors. Advances in Pharmacology* vol. 80 (Elsevier Inc., 2017).
77. Bouaboula, M. *et al.* Anandamide induced PPAR γ transcriptional activation and 3T3-L1 preadipocyte differentiation. *Eur. J. Pharmacol.* **517**, 174–181 (2005).
78. Benjamin F. Cravatt *et al.* Molecular characterization of an enzyme that degrades neuromodulatory fatty-acid amides. *Nature* **384**, 83–87 (1996).
79. Dinh, T. P. *et al.* Brain monoglyceride lipase participating in endocannabinoid inactivation. *Proc. Natl. Acad. Sci. U. S. A.* **99**, 10819–10824 (2002).
80. Devane, W. A., Dysarz, F. A., Johnson, M. R., Melvin, L. S. & Howlett, A. C. Determination and characterization of a cannabinoid receptor in rat brain. *Mol. Pharmacol.* **34**, 605–613 (1988).
81. Matsuda, L. A., Lolait, S. J., Brownstein, M. J., Young, A. C. & Bonner, T. I. Structure of a cannabinoid receptor and functional expression of the cloned cDNA. *Nature* **346**, 561–564 (1990).
82. Munro, S., Thomas, K. L. & Abu-Shaar, M. Molecular characterization of a peripheral receptor for cannabinoids. *Nature* **365**, 61–65 (1993).
83. Varvel, S. A. *et al.* Δ^9 -tetrahydrocannabinol accounts for the antinociceptive, hypothermic, and cataleptic effects of marijuana in mice. *J. Pharmacol. Exp. Ther.* **314**, 329–337 (2005).

84. Derkinderen, P., Ledent, C., Parmentier, M. & Girault, J. A. Cannabinoids activate p38 mitogen-activated protein kinases through CB1 receptors in hippocampus. *J. Neurochem.* **77**, 957–960 (2001).
85. Dalton, G., Bass, C., Van Horn, C. & Howlett, A. Signal transduction via cannabinoid receptors. *CNS Neurol. Disord. - Drug Targets* **8**, 422–431 (2012).
86. Marsicano, G. & Lutz, B. Expression of the cannabinoid receptor CB1 in distinct neuronal subpopulations in the adult mouse forebrain. *Eur. J. Neurosci.* **11**, 4213–4225 (1999).
87. Onaivi, E. S., Ishiguro, H., Gu, S. & Liu, Q. R. CNS effects of CB2 cannabinoid receptors: beyond neuro-immuno-cannabinoid activity. *J. Psychopharmacol.* **26**, 92–103 (2012).
88. Mackie, K. Distribution of Cannabinoid Receptors in the Central and Peripheral Nervous System. in *Handbook of Experimental Pharmacology* 299–325 (2005).
89. Chiarlone, A. *et al.* A restricted population of CB1 cannabinoid receptors with neuroprotective activity. *Proc. Natl. Acad. Sci. U. S. A.* **111**, 8257–8262 (2014).
90. Albayram, O. *et al.* Role of CB1 cannabinoid receptors on GABAergic neurons in brain aging. *Proc. Natl. Acad. Sci. U. S. A.* **108**, 11256–11261 (2011).
91. Trillou, C. R., Delgorge, C., Menet, C., Arnone, M. & Soubrie, P. CB1 cannabinoid receptor knockout in mice leads to leanness, resistance to diet-induced obesity and enhanced leptin sensitivity. *Int. J. Obes.* **28**, 640–648 (2004).
92. Cota, D. *et al.* The endogenous cannabinoid system affects energy balance via central orexigenic drive and peripheral lipogenesis. *J. Clin. Invest.* **112**, 423–431 (2003).

93. Jourdan, T. *et al.* CB1 antagonism exerts specific molecular effects on visceral and subcutaneous fat and reverses liver steatosis in diet-induced obese mice. *Diabetes* **59**, 926–934 (2010).
94. Simard, G. & Malthie, Y. Effects of the cannabinoid CB1 antagonist rimonabant on hepatic mitochondrial function in rats fed a high-fat diet. *Am. J. Physiol. Endocrinol. Metab.* **297**, 1162–1170 (2009).
95. Koch, M. *et al.* Hypothalamic POMC neurons promote cannabinoid-induced feeding. *Nature* **519**, 45–50 (2015).
96. Osei-Hyiaman, D. *et al.* Hepatic CB 1 receptor is required for development of diet-induced steatosis, dyslipidemia, and insulin and leptin resistance in mice. *J. Clin. Invest.* **118**, 3160–3169 (2008).
97. Juan-pic, P. *et al.* Cannabinoid receptors regulate Ca²⁺ signals and insulin secretion in pancreatic β -cell. *Cell Calcium* **39**, 155–162 (2006).
98. Cavauto, P. *et al.* The expression of receptors for endocannabinoids in human and rodent skeletal muscle. *Biochem. Biophys. Res. Commun.* **364**, 105–110 (2007).
99. Lipina, C., Irving, A. J. & Hundal, H. S. Mitochondria: a possible nexus for the regulation of energy homeostasis by the endocannabinoid system? *Am. J. Physiol. Endocrinol. Metab.* **307**, E1–E13 (2014).
100. Bénard, G. *et al.* Mitochondrial CB 1 receptors regulate neuronal energy metabolism. *Nat. Neurosci.* **15**, 558–564 (2012).

101. Hebert-Chatelain, E. *et al.* A cannabinoid link between mitochondria and memory. *Nature* **539**, 555–559 (2016).
102. Purdon, A. D., Rosenberger, T. A., Shetty, H. U. & Rapoport, S. I. Energy consumption by phospholipid metabolism in mammalian brain. *Neurochem. Res.* **27**, 1641–1647 (2002).
103. Bilkei-Gorzo, A. *et al.* Early age-related cognitive impairment in mice lacking cannabinoid CB1 receptors. *Proc. Natl. Acad. Sci. U. S. A.* **102**, 15670–15675 (2005).
104. Wood-Kaczmar, A. *et al.* PINK1 is necessary for long term survival and mitochondrial function in human dopaminergic neurons. *PLoS One* **3**, e2455 (2008).
105. Lazarou, M. *et al.* The ubiquitin kinase PINK1 recruits autophagy receptors to induce mitophagy. *Nature* **524**, 309–314 (2015).
106. Srivastava, S. The mitochondrial basis of aging and age-related disorders. *Genes (Basel)*. **8**, 1–23 (2017).
107. Hämäläinen, R. R. H. *et al.* Tissue- and cell-type-specific manifestations of heteroplasmic mtDNA 3243A>G mutation in human induced pluripotent stem cell-derived disease model. *Proc. Natl. Acad. Sci. U. S. A.* **110**, E3622–E3630 (2013).
108. Matsuda, N. *et al.* PINK1 stabilized by mitochondrial depolarization recruits Parkin to damaged mitochondria and activates latent Parkin for mitophagy. *J. Cell Biol.* **189**, 211–221 (2010).
109. Narendra, D. P. *et al.* PINK1 is selectively stabilized on impaired mitochondria to activate Parkin. *PLoS Biol.* **8**, e1000298 (2010).

110. Jin, S. M. *et al.* Mitochondrial membrane potential regulates PINK1 import and proteolytic destabilization by PARL. *J. Cell Biol.* **191**, 933–942 (2010).
111. Koyano, F. *et al.* Ubiquitin is phosphorylated by PINK1 to activate parkin. *Nature* **510**, 162–166 (2014).
112. Kane, L. A. *et al.* PINK1 phosphorylates ubiquitin to activate Parkin E3 ubiquitin ligase activity. *J. Cell Biol.* **205**, 143–153 (2014).
113. Kazlauskaitė, A. *et al.* Parkin is activated by PINK1-dependent phosphorylation of ubiquitin at Ser 65. *Biochem. J.* **139**, 127–139 (2014).
114. Iguchi, M. *et al.* Parkin-catalyzed ubiquitin-ester transfer is triggered by PINK1-dependent phosphorylation. *J. Biol. Chem.* **288**, 22019–22032 (2013).
115. Shiba-fukushima, K., Imai, Y., Yoshida, S., Ishihama, Y. & Kanao, T. PINK1-mediated phosphorylation of the Parkin ubiquitin-like domain primes mitochondrial translocation of Parkin and regulates mitophagy. *Sci. Rep.* **2**, 1002 (2012).
116. Zhang, N. *et al.* PINK1 is activated by mitochondrial membrane potential depolarization and stimulates Parkin E3 ligase activity by phosphorylating Serine 65. *Open Biol.* **2**, 120080 (2012).
117. Mcwilliams, T. G. *et al.* Phosphorylation of Parkin at serine 65 is essential for its activation in vivo. *Open Biol.* **8**, 180108 (2018).
118. Cornelissen, T. *et al.* Deficiency of parkin and PINK1 impairs age-dependent mitophagy in *Drosophila*. *Elife* **7**, e35878 (2018).

119. Park, J. *et al.* Mitochondrial dysfunction in *Drosophila* PINK1 mutants is complemented by parkin. *Nature* **441**, 1157–1161 (2006).
120. Whitworth, A. J. *et al.* Increased glutathione S-transferase activity rescues dopaminergic neuron loss in a *Drosophila* model of Parkinson's disease. *Proc. Natl. Acad. Sci. U. S. A.* **102**, 8024–8029 (2005).
121. Shiba-Fukushima, K. *et al.* Evidence that phosphorylated ubiquitin signaling is involved in the etiology of Parkinson's disease. *Hum. Mol. Genet.* **26**, 3172–3185 (2017).
122. Fiesel, F. C. *et al.* (Patho-)physiological relevance of PINK 1 -dependent ubiquitin phosphorylation. *EMBO Rep.* **16**, 1114–1130 (2015).
123. Hou, X. *et al.* Age- and disease-dependent increase of the mitophagy marker phospho-ubiquitin in normal aging and Lewy body disease. *Autophagy* **14**, 1404–1418 (2018).
124. McWilliams, T. G. *et al.* Basal mitophagy occurs independently of PINK1 in mouse tissues of high metabolic demand. *Cell Metab.* **27**, 1–11 (2018).
125. McWilliams, T. G. *et al.* Mito-QC illuminates mitophagy and mitochondrial architecture in vivo. *J. Cell Biol.* **214**, 333–345 (2016).
126. Hernandez, G. *et al.* MitoTimer: a novel tool for monitoring mitochondrial turnover. *Autophagy* **9**, 1852–1861 (2013).
127. Sliter, D. A. *et al.* Parkin and PINK1 mitigate STING-induced inflammation. *Nature* **561**, 258–262 (2018).

128. Kataoka, K., Bilkei-Gorzo, A., Zimmer, A. & Asahi, T. Immunohistochemical characterization of phosphorylated ubiquitin in the mouse hippocampus. *bioRxiv* (2020) doi:<https://doi.org/10.1101/2020.01.20.912238>.
129. Pereira, J. B. *et al.* Regional vulnerability of hippocampal subfields and memory deficits in Parkinson's disease. *Hippocampus* **728**, 720–728 (2013).
130. Tanner, J. J., Mcfarland, N. R., Price, C. C. & Price, C. C. Striatal and hippocampal atrophy in idiopathic Parkinson's disease patients without dementia: a morphometric analysis. *Front. Neurol.* **8**, 139 (2017).
131. Taymans, J. M., Van Den Haute, C. & Baekelandt, V. Distribution of PINK1 and LRRK2 in rat and mouse brain. *J. Neurochem.* **98**, 951–961 (2006).
132. Blackinton, J. G. *et al.* Expression of PINK1 mRNA in human and rodent brain and in Parkinson's disease. *Brain Res.* **1184**, 10–16 (2007).
133. Fang, E. F. *et al.* NAD⁺ replenishment improves lifespan and healthspan in ataxia telangiectasia models via mitophagy and DNA repair. *Cell Metab.* **24**, 566–581 (2016).
134. Fang, E. F. *et al.* Defective mitophagy in XPA via PARP-1 hyperactivation and NAD⁺/SIRT1 reduction. *Cell* **157**, 882–896 (2014).
135. Agnihotri, S. K., Shen, R., Li, J., Gao, X. & Büeler, H. Loss of PINK1 leads to metabolic deficits in adult neural stem cells and impedes differentiation of newborn neurons in the mouse hippocampus. *FASEB J.* **31**, 2839–2853 (2017).

136. Piomelli, D. The molecular logic of endocannabinoid signalling. *Nat. Rev. Neurosci.* **4**, 873–884 (2003).
137. Piyanova, A. *et al.* Age-related changes in the endocannabinoid system in the mouse hippocampus. *Mech. Ageing Dev.* **150**, 55–64 (2015).
138. Wang, L., Liu, J., Harvey-White, J., Zimmer, A. & Kunos, G. Endocannabinoid signaling via cannabinoid receptor 1 is involved in ethanol preference and its age-dependent decline in mice. *Proc. Natl. Acad. Sci. U. S. A.* **100**, 1393–1398 (2003).
139. Albayram, O., Bilkei-Gorzo, A. & Zimmer, A. Loss of CB1 receptors leads to differential age-related changes in reward-driven learning and memory. *Front. Aging Neurosci.* **4**, 34 (2012).
140. Bilkei-Gorzo, A. *et al.* A chronic low dose of Δ^9 -tetrahydrocannabinol (THC) restores cognitive function in old mice. *Nat. Med.* **23**, 782–787 (2017).
141. Han, J. *et al.* Acute cannabinoids impair working memory through astroglial CB 1 receptor modulation of hippocampal LTD. *Cell* **148**, 1039–1050 (2012).
142. Bartova, A. & Birmingham, M. K. Effect of Δ^9 -tetrahydrocannabinol on mitochondrial NADH-oxidase activity. *J. Biol. Chem.* **251**, 5002–5006 (1976).
143. Fonseca, B. M., Correia-da-Silva, G. & Teixeira, N. A. The endocannabinoid anandamide induces apoptosis of rat decidual cells through a mechanism involving ceramide synthesis and p38 MAPK activation. *Apoptosis* **18**, 1526–1535 (2013).

144. Athanasiou, A. *et al.* Cannabinoid receptor agonists are mitochondrial inhibitors: a unified hypothesis of how cannabinoids modulate mitochondrial function and induce cell death. *Biochem. Biophys. Res. Commun.* **364**, 131–137 (2007).
145. Sarafian, T. A. *et al.* Δ^9 -Tetrahydrocannabinol disrupts mitochondrial function and cell energetics. *Am. J. Physiol. Cell. Mol. Physiol.* **90095**, 298–306 (2002).
146. Tedesco, L. *et al.* Cannabinoid receptor stimulation impairs mitochondrial biogenesis in mouse white adipose tissue, muscle, and liver: the role of eNOS, p38 MAPK, and AMPK pathways. *Diabetes* **59**, 2826–2836 (2010).
147. Catanzaro, G., Rapino, C., Oddi, S. & Maccarrone, M. Anandamide increases swelling and reduces calcium sensitivity of mitochondria. *Biochem. Biophys. Res. Commun.* **388**, 439–442 (2009).
148. Mendizabal-Zubiaga, J. *et al.* Cannabinoid CB1 receptors are localized in striated muscle mitochondria and regulate mitochondrial respiration. *Front. Physiol.* **7**, 476 (2016).
149. Kataoka, K. *et al.* Age-dependent alteration in mitochondrial dynamics and autophagy in hippocampal neuron of cannabinoid CB1 receptor-deficient mice. *Brain Res. Bull.* **140**, 40–49 (2020).
150. Sheng, Z. H. & Cai, Q. Mitochondrial transport in neurons: impact on synaptic homeostasis and neurodegeneration. *Nat. Rev. Neurosci.* **13**, 77–93 (2012).

151. Davies, V. J. *et al.* OPA1 deficiency in a mouse model of autosomal dominant optic atrophy impairs mitochondrial morphology, optic nerve structure and visual function. *Hum. Mol. Genet.* **16**, 1307–1318 (2007).
152. Ishihara, N. *et al.* Mitochondrial fission factor Drp1 is essential for embryonic development and synapse formation in mice. *Nat. Cell Biol.* **11**, 958–966 (2009).
153. Morozov, Y. M., Datta, D., Paspalas, C. D. & Arnsten, A. F. T. Ultrastructural evidence for impaired mitochondrial fission in the aged rhesus monkey dorsolateral prefrontal cortex. *Neurobiol. Aging* **51**, 9–18 (2017).
154. Chen, H. *et al.* Mitochondrial fusion is required for mtDNA stability in skeletal muscle and tolerance of mtDNA mutations. *Cell* **141**, 280–289 (2010).
155. Sebastián, D., Hernández-alvarez, M. I., Segalés, J. & Sorianoello, E. Mitofusin 2 (Mfn2) links mitochondrial and endoplasmic reticulum function with insulin signaling and is essential for normal glucose homeostasis. *Proc. Natl. Acad. Sci. U. S. A.* **109**, 5523–5528 (2012).
156. Vincent, A. E., Turnbull, D. M., Eisner, V., Hajnóczky, G. & Picard, M. Mitochondrial nanotunnels. *Trends Cell Biol.* **27**, 787–799 (2017).
157. Vincent, A. E. *et al.* Quantitative 3D mapping of the human skeletal muscle mitochondrial network. *Cell Rep.* **26**, 996-1009.e4 (2019).
158. Zhang, L. *et al.* Altered brain energetics induces mitochondrial fission arrest in Alzheimer's disease. *Sci. Rep.* **6**, 18725 (2016).

159. Trushina, E. *et al.* Defects in mitochondrial dynamics and metabolomic signatures of evolving energetic stress in mouse models of familial Alzheimer's disease. *PLoS One* **7**, e32737 (2012).
160. Piyanova, A. *et al.* Loss of CB1 receptors leads to decreased cathepsin D levels and accelerated lipofuscin accumulation in the hippocampus. *Mech. Ageing Dev.* **134**, 391–399 (2013).
161. McCoy, M. K., Kaganovich, A., Rudenko, I. N., Ding, J. & Cookson, M. R. Hexokinase activity is required for recruitment of parkin to depolarized mitochondria. *Hum. Mol. Genet.* **23**, 145–156 (2014).
162. Soutar, M. P. M. *et al.* AKT signalling selectively regulates PINK1 mitophagy in SHSY5Y cells and human iPSC-derived neurons. *Sci. Rep.* **8**, 8855 (2018).
163. Ruhl, T. *et al.* Acute administration of THC impairs spatial but not associative memory function in zebrafish. *Psychopharmacology (Berl)*. **231**, 3829–3842 (2014).
164. Huang, N. *et al.* Rimonabant inhibits TNF- α -induced endothelial IL-6 secretion via CB1 receptor and cAMP-dependent protein kinase pathway. *Acta Pharmacol. Sin.* **31**, 1447–1453 (2010).
165. Di Rita, A. *et al.* HUWE1 E3 ligase promotes PINK1/PARKIN-independent mitophagy by regulating AMBRA1 activation via IKK α . *Nat. Commun.* **9**, 3755 (2018).
166. Laforge, M. *et al.* NF- κ B pathway controls mitochondrial dynamics. *Cell Death Differ.* **23**, 89–98 (2016).

167. Shields, L. Y. *et al.* Dynamin-related protein 1 is required for normal mitochondrial bioenergetic and synaptic function in CA1 hippocampal neurons. *Cell Death Dis.* **6**, e1725 (2015).
168. Cribbs, J. T. & Strack, S. Reversible phosphorylation of Drp1 by cyclic AMP-dependent protein kinase and calcineurin regulates mitochondrial fission and cell death. *EMBO Rep.* **8**, 939–944 (2007).
169. Chang, C. R. & Blackstone, C. Cyclic AMP-dependent protein kinase phosphorylation of Drp1 regulates its GTPase activity and mitochondrial morphology. *J. Biol. Chem.* **282**, 21583–21587 (2007).
170. Drori, A. *et al.* Cannabinoid-1 receptor regulates mitochondrial dynamics and function in renal proximal tubular cells. *Diabetes Obes. Metab.* **21**, 146–159 (2019).
171. Rambold, A. S., Kostelecky, B., Elia, N. & Lippincott-Schwartz, J. Tubular network formation protects mitochondria from autophagosomal degradation during nutrient starvation. *Proc. Natl. Acad. Sci. U. S. A.* **108**, 10190–10195 (2011).
172. Song, M. & Dorn II, G. W. Mitoconfusion: noncanonical functioning of dynamism factors in static mitochondria of the heart. *Cell Metab.* **21**, 195–205 (2015).
173. Amer, Y. O. & Hebert-chatelain, E. Mitochondrial cAMP-PKA signaling: what do we really know? *Biochim. Biophys. Acta - Bioenerg.* **1859**, 868–877 (2018).
174. Akabane, S. *et al.* PKA regulates PINK1 stability and Parkin recruitment to damaged mitochondria through phosphorylation of MIC60. *Mol. Cell* **62**, 371–384 (2016).

175. Bilkei-Gorzo, A. *et al.* Early onset of aging-like changes is restricted to cognitive abilities and skin structure in *Cnr1*^{-/-}-mice. *Neurobiol. Aging* **33**, e11–e22 (2012).
176. Todorova, V. & Blokland, A. Mitochondria and synaptic plasticity in the mature and aging nervous system. *Curr. Neuropharmacol.* **15**, 166–173 (2017).
177. Brot, S. *et al.* Collapsin response mediator protein 5 (CRMP5) induces mitophagy, thereby regulating mitochondrion numbers in dendrites. *J. Biol. Chem.* **289**, 2261–2276 (2014).
178. Cherra, S. J., Steer, E., Gusdon, A. M., Kiselyov, K. & Chu, C. T. Mutant LRRK2 elicits calcium imbalance and depletion of dendritic mitochondria in neurons. *Am. J. Pathol.* **182**, 474–484 (2013).
179. Laplante, M. & Sabatini, D. M. mTOR signaling in growth control and disease. *Cell* **149**, 274–293 (2012).
180. Younts, T. J. *et al.* Presynaptic protein synthesis is required for long-term plasticity of GABA release. *Neuron* **92**, 479–492 (2016).
181. Wyant, G. A. *et al.* Nufip1 is a ribosome receptor for starvation-induced ribophagy. *Science* (80-.). **360**, 751–758 (2018).
182. Turi, Z., Lacey, M., Mistrik, M. & Moudry, P. Impaired ribosome biogenesis: mechanisms and relevance to cancer and aging. *Aging (Albany. NY)*. **11**, 2512–2540 (2019).
183. McPartland, J., Marzo, V. Di, De Petrocellis, L., Mercer, A. & Glass, M. Cannabinoid receptors are absent in insects. *J. Comp. Neurol.* **436**, 423–429 (2001).

184. Mcpartland, J. M., Matias, I., Di, V. & Glass, M. Evolutionary origins of the endocannabinoid system. *Gene* **370**, 64–74 (2006).
185. Riddle, M. R. *et al.* Insulin resistance in cavefish as an adaptation to a nutrient-limited environment. *Nature* **555**, 647–651 (2018).
186. Strickler, A. G. & Soares, D. Comparative genetics of the central nervous system in epigeal and hypogean *Astyanax mexicanus*. *Genetica* **139**, 383–391 (2011).
187. Edrey, Y. H. *et al.* Amyloid beta and the longest-lived rodent: the naked mole-rat as a model for natural protection from Alzheimer's disease. *Neurobiol. Aging* **34**, 2352–2360 (2013).

Acknowledgement

First of all, I would like to thank thesis committee: **Professor Toru Asahi, Professor Andreas Zimmer, Professor Haruko Takeyama** and **Professor Shinji Takeoka** for their insightful comments, suggestions and encouragements.

I would like to express my deepest appreciation to my supervisor, **Professor Toru Asahi**, for encouraging me all the time during my doctoral program and offering me a variety of great opportunities including this research projects. He has also encouraged and motivated me in various situations since my undergraduate years. Invaluable time with him included midnight karaoke party. His presence has greatly expanded my philosophy of career and life in various respects.

I would also like to appreciate continuous supports from **Dr. Andras Bilkei-Gorzo** and **Dr. Chihiro Nozaki** in University of Bonn. They always motivated me to conduct the project involving this thesis, and gave me a number of scientific advices. They also kindly share their experience and knowledge on the scientific careers and experimental techniques, which make them great mentors for me. I could not have imagined completed this thesis without them.

I am also grateful to all members and staffs of Zimmer lab and Asahi lab. I would like to mention a special thanks to **Ms. Edda Erxlebe, Ms. Kerstin Nicolai, Ms. Joanna Koromowska, Ms. Aiko Maeda** and **Ms. Hisae Nakanishi**, for their advices and supports of laboratory experiments, general affairs and private things.

My sincere thanks also go to **Dr. Chihiro Nozaki, Mr. Hidetoshi Takahashi** and **Ms. Maya Takahashi**. They kindly took me many places in city of Bonn, such as supermarkets and

restaurants, and provided me precious time there. They also warmly cooked me dinners many times in their house, which helped me to survive in Germany. The time shared with them will be one of the great memories in my life in Bonn.

I would like to express my gratitude to **Professor Keisuke Ohta, Professor Keiichiro Nakamura** and **Mr. Akinobu Togo** in Kurume University, Fukuoka, Japan. They technically supported my project in electron microscopy, and gave me insightful suggestions and comments. They also introduced many great restaurants in city of Kurume in Fukuoka to me, which motivated me to work hard in the new field.

I would also like to thank **Dr. Nils Gassen** in University of Bonn for insightful discussions. He gave me numerous novel ideas on biology, and kindly offered me a great chance to conduct the next project involving this thesis.

I would also like to appreciate **all of members in cricket genome project**. They offered me novel and intriguing scientific perspectives on biology. This project team will bring me exciting ideas from now on too.

I am also thankful to **all of my friends**. They encouraged and enlightened me all the time. They went out with me for eating and drinking even in the midnight when they and I were feeling like crazy. This might make anabolic state dominate in my body.

Finally, I would like to express a deep sense of my gratitude to my parents, **Takafumi** and **Mika**, for unconditionally supporting me during my life. Their support always encouraged me and helped my life in Tokyo. I also appreciate their patience and generosity for my career.

This study is financially supported by The Top Global University Project and JSPS
KAKENHI (Grant number: 19K20196 and JP16H06280) from MEXT, Japan.

早稲田大学 博士（理学） 学位申請 研究業績書

氏名 片岡 孝介 印

(2020 年 4 月 現在)

種 類 別	題名、 発表・発行掲載誌名、 発表・発行年月、 連名者（申請者含む）
論文	○ Kataoka, K. , Bilkei-Gorzo, A., Nozaki, C., Togo, A., Nakamura, K., Ohta, K., Zimmer, A., Asahi, T. “Age-dependent alteration in mitochondrial dynamics and autophagy in hippocampal neuron of cannabinoid CB1 receptor-deficient mice”, <i>Brain Research Bulletin</i> , in press, DOI: 10.1016/j.brainresbull.2020.03.014 (2020).
講演	片岡孝介, Andras Bilkei-Gorzo, Andreas Zimmer, 朝日透, 「カンナビノイド受容体 CB1 の海馬内ミトファジーへの関与」, 第 18 回日本ミトコンドリア学会年会, 久留米, 福岡, 2018 年 12 月. Kataoka, K. , Bilkei-Gorzo, A., Nidadavolu, P., Nozaki, C., Zimmer, A., Asahi, T. “Mitophagy in hippocampal pyramidal neurons is reduced by cannabinoid receptor CB1 deficiency”, Cluster Science Day 2018 and the 10 th International Symposium of IFRcC, Bonn, Germany, November 2018. Kataoka, K. , Bilkei-Gorzo, A., Zimmer, A., Asahi, T. “Brain ageing from the points of mitochondria and cannabinoid”, MIRAI Ageing Workshop, Gothenburg, Sweden, June 2018. Kataoka, K. , Bilkei-Gorzo, A., Zimmer, A., Asahi, T. “Cannabinoid receptor 1 deletion leads to reduction in phosphorylated ubiquitin in hippocampal pyramidal cell layer”, 4 th Core-to-Core International Symposium, Bonn, Germany, March 2018.
その他 (論文)	Kataoka, K. , Minei, R., Ide, K., Ogura, A., Takeyama, H., Takeda, M., Suzuki, T., Yura, K., Asahi, T. “The Draft Genome Dataset of the Asian Cricket <i>Teleogryllus occipitalis</i> for Molecular Research toward Entomophagy”, <i>Frontiers in Genetics</i> , in press, DOI: 10.3389/fgene.2020.00470 (2020) Kataoka, K. , Bilkei-Gorzo, A., Zimmer, A., Asahi, T. “Immunohistochemical characterization of phosphorylated ubiquitin in the mouse hippocampus”, <i>bioRxiv</i> , DOI: 10.1101/2020.01.20.912238 (2020). Wada, T., Hanyu, T., Nozaki, K., Kataoka, K. , Kawatani, T., Asahi, T., Sawamura, N. “Antioxidant activity of Ge-132, a synthetic organic germanium, on cultured mammalian cells”, <i>Biological and Pharmacological Bulletin</i> 41 (5), 749-753, DOI: 10.1248/bpb.b17-00949 (2018). Kataoka, K. , Nakamura, C., Asahi, T., Sawamura, N. “Mitochondrial cereblon functions as a Lon-type protease”, <i>Scientific Reports</i> 6 , 29986, DOI: 10.1038/srep29986 (2016).
その他 (講演)	片岡孝介, 嶺井隆平, 井手圭吾, 小倉淳, 竹山春子, 竹田真木生, 鈴木丈詞, 由良敬, 朝日透, 「タイワンエンマコオロギの全ゲノム塩基配列解読: 大量生産に向けた高効率品種改良技術の幕開け」, 第 64 回応用動物昆虫学会大会, 名古屋, 2020 年 3 月. 片岡孝介, 朝日透, 澤村直哉, “Cereblon promotes mitochondrial degradation via autophagy in human neuroblastoma cells”, 第 60 回日本神経化学学会大会, 仙台, 2017 年 9 月. Kataoka, K. , Asahi, T., Sawamura, N. “Cereblon promotes mitophagy in human neuroblastoma cells”, The 8th International Symposium on Autophagy, Nara, Japan, May 2017.

早稲田大学 博士（理学） 学位申請 研究業績書

種 類 別	題名、 発表・発行掲載誌名、 発表・発行年月、 連名者（申請者含む）
その他 (講演)	<p>片岡孝介, 朝日透, 澤村直哉, 「Cereblon の Lon protease としての機能解析」, 第 39 回日本分子生物学会年会, 神奈川, 2016 年 11 月.</p> <p>片岡孝介, 「皮膚健康モニタリングにむけた EDGE プログラムでの取り組み」, 平成 28 年度 WASEDA-EDGE 人材育成プログラムシンポジウム 受講生成果報告, 2016 年 12 月.</p> <p><u>Kataoka, K.</u>, Asahi, T., Sawamura, N. “The Role of Cereblon as s Lon-type protease”, The 13th conference of Asian Society for Mitochondrial Research and Medicine [ASMRM] The 16th Conference of Japanese Society of Mitochondrial Research and Medicine [J-mit], Tokyo, Japan, October 2016.</p> <p>片岡孝介, 朝日透, 澤村直哉, 「Cereblon の Lon protease としての役割」, 第 15 回日本ミトコンドリア学会年会, 福井, 2015 年 11 月.</p> <p>片岡孝介, 朝日透, 澤村直哉, “Mitochondria-targeted cereblon suppressed stress-induced cell death”, 第 58 回日本神経化学学会大会, 埼玉, 2015 年 9 月.</p> <p>片岡孝介, 丸山祐丞, 島岡未来子, 大橋啓之, 「動物生体バランス」, 第 3 回 EDGE プログラムシンポジウム DEMO DAY, 東京, 2015 年 9 月.</p> <p>片岡孝介, 朝日透, 澤村直哉, 「精神遅滞候補遺伝子産物セレブロン/mitochondriaにおける機能解析」, 第 67 回日本細胞生物学会大会, 東京, 2015 年 7 月.</p> <p><u>Kataoka, K.</u>, Asahi, T., Sawamura, N. “Functional analysis of mitochondria-targeted cereblon”, The 16th Joint Symposium between the University of Bonn and Waseda University, Tokyo, Japan, February 2015.</p> <p><u>Kataoka, K.</u>, Asahi, T., Sawamura, N. “Functional analysis of cereblon protein in mitochondria”, EMNT2014 10th International Symposium on Electrochemical Micro and Nanosystem Technologies, Okinawa, Japan, November 2014.</p> <p><u>Kataoka, K.</u>, Asahi, T., Sawamura, N. “Functional analysis of cereblon, a candidate gene product for intellectual disability, in mitochondria”, Three-Dimensional Development of Lab-Exchange Type Biomedical Science Research Consortium, Chiba, Japan, September 2014.</p>

早稲田大学 博士（理学） 学位申請 研究業績書

種 類 別	題名、 発表・発行掲載誌名、 発表・発行年月、 連名者（申請者含む）
その他 (受賞)	<p>神経化学教育口演優秀発表賞，<u>片岡孝介</u>，朝日透，澤村直哉，“Mitochondria-targeted cereblon suppressed stress-induced cell death”，第58回日本神経化学会大会，埼玉，2015年9月.</p> <p>最優秀賞，<u>片岡孝介</u>，丸山祐丞，島岡未来子，大橋啓之，「動物生体バランス」，第3回EDGEプログラムシンポジウム DEMO DAY，東京，2015年9月.</p>